**Article:**

Gegg, Lukas, Jacob, Laura, Moine, Olivier et al. (7 more authors) (2024) Climatic and tectonic controls on deposition in the Heidelberg Basin, Upper Rhine Graben, Germany. Quaternary Science Reviews. 109018. ISSN 0277-3791

https://doi.org/10.1016/j.quascirev.2024.109018

# Climatic and tectonic controls on deposition in the Heidelberg Basin, Upper Rhine Graben, Germany

Lukas Gegg [a],[*], Laura Jacob [a], Olivier Moine [b], Ellie Nelson [c], Kirsty E.H. Penkman [c], Fiona Schwahn [a], Philipp Stojakowits [d], Dustin White [c], Ulrike Wielandt-Schuster [e], Frank Preusser [a]

[a] Institute of Earth and Environmental Sciences, University of Freiburg, Albertstraße 23b, 79104, Freiburg, Germany
[b] Laboratoire de Géographie Physique, UMR 8591 CNRS-Université Paris 1-UPEC, 2 Rue Henri Dunant, 94320, Thiais, France
[c] Department of Chemistry, University of York, Heslington, York, YO10 5DD, United Kingdom
[d] Landesamt für Bergbau, Energie und Geologie (LBEG) and Bundesanstalt für Geowissenschaften und Rohstoffe (BGR), Stilleweg 2, 30655 Hannover, Germany, and Institute of Geography, University of Augsburg, Alter Postweg 118, 86159, Augsburg, Germany
[e] Regierungspräsidium Freiburg, Landesamt für Geologie, Rohstoffe und Bergbau (LGRB), Albertstraße 5, 79104, Freiburg, Germany

## ARTICLE INFO

## ABSTRACT

The Upper Rhine Graben in Central Europe, and notably its depocentre in the Heidelberg Basin, is an archive of complex and long-lasting deposition throughout the Quaternary. A new drill core, 136 m long, from the southern Heidelberg Basin is investigated by characterising sedimentary facies, sediment provenance, as well as analysing the pollen and mollusc content. The chronological framework is based on post-infrared infrared-stimulated luminescence dating, and complemented with amino acid geochronology. The sediment sequence consists of fluvial, colluvial, and palustrine deposits that represent at least the last ~500 ka, interrupted by some, major and minor, hiatuses. In the lower part, fluvial gravel and colluvial diamicts of a lateral alluvial fan into the Upper Rhine Graben prevail. The central part of the succession consists of a large-scale fining upward cycle that contains increasing amounts of material from the Alps delivered by the Rhine river. This sequence terminates with palustrine fines with rich mollusc and pollen assemblages that allow for a detailed reconstruction of environmental conditions. The results of pIRIR dating place the palustrine deposits in marine isotope stage 11. However, the pollen profile shares similarities with the Mannheim Interglacial that has previously been assigned to the Cromerian, a correlation that is supported by the amino acid geochronology, which poses a chronostratigraphical problem. In the upper part, Alpine sediments are progressively replaced by a new alluvial fan from the graben margin with striking variations in grain size. Overall, the diverse succession is the result of an interplay of tectonic activity and climatic factors. While subsidence triggers the generation of accommodation space and river deflection, pulses of coarse sediment are probably related to periglacial weathering, mass wasting and short-scale transport during cold periods.

## 1. Introduction

Past climate change as well as tectonic processes have played a key role in the shaping of the surface of the Earth and governed the distribution of sediments (e.g. Jansen et al., 2007; Szymanek and Julien, 2018; Gibbard and Hughes, 2021). However, on the continents, sedimentary products of terrestrial geomorphological processes are only sporadically and fragmentarily preserved for longer timescales, as erosion and sediment transport usually outweigh deposition

(Schlüchter, 1992; Holland, 2016; Hughes et al., 2019; Gibbard and Hughes, 2021). Continuous deposition and a high preservation potential can be encountered in subsiding basins, resulting in sedimentary archives that stretch over long periods of time. However, as these are often only accessible through costly drilling operations, the availability of information from such archives is rather limited and must be fully exploited.

One noteworthy large-scale and long-term sediment sink is the Upper Rhine Graben (URG) in southwestern Central Europe, a failed rift basin

stretching over >350 km from the SSW to the NNE (Fig. 1). As part of the European Cenozoic Rift System (Ziegler, 1992; Dèzes et al., 2004), its formation began in the Paleogene, and the graben has since been episodically subsiding and acting as a sediment trap (Berger et al., 2005). The main depocentre is the Heidelberg Basin in the northeastern sector of the graben, which hosts up to ~500 m of Quaternary deposits (Bartz, 1974; Hagedorn and Boenigk, 2008; Gabriel et al., 2013). With its unconsolidated sediment fill consisting to a large extent of permeable gravel and sand, the URG is a regionally significant groundwater reservoir (Meinken and Stober, 1997; Wirsing and Luz, 2007; Koltzer et al., 2019). Due to the steep geothermal gradient, it is also a promising target for geothermal exploration (Stober and Bucher, 2015; Frey et al., 2022). Potential reservoirs for deep carbon storage (e.g. Beccaletto et al., 2010) and records of palaeoseismicity in a tectonically active setting (e. g. Ritter et al., 2009; Pena-Castellnou et al., 2023) are further applied aspects motivating research. From an academic standpoint, the deposits trapped in the URG (and specifically in the Heidelberg Basin) contain ample information of geomorphic processes in the graben and its tributary catchments (e.g. Ellwanger et al., 2005, 2011; Gabriel et al., 2013, and references therein), and of ecosystems and environmental conditions (e.g. Bos et al., 2008; Knipping, 2008; Wedel, 2009) as well. Moreover, insights into the recent evolution of the URG can help to bridge the gap between the areas affected by repeated Alpine and Fennoscandian glaciations respectively (Gabriel et al., 2013; Bittmann et al., 2018), i.e. the northern Alpine foreland (e.g. Penck and Brückner, 1909; Ellwanger et al., 2011; Schlüchter et al., 2021) and the lowlands of northern Central Europe (e.g. Keilhack, 1915; Litt et al., 2007; Böse et al., 2012).

We present here a new stratigraphic profile from the Heidelberg Basin, the main depocentre of the only sporadically investigated URG. As a hotspot of subsidence from the Pliocene until nowaday, it is infilled by diverse fluvial, colluvial, and palustrine sediments, which are here recovered in a 136-m-long drill core. We investigate the sedimentary lithofacies and provenance in light of the regional tectonic setting, and with a variety of sedimentological and stratigraphical methods. In selected sections the fossil mollusc and pollen contents are determined, and provide information on biostratigraphy and environmental conditions. Our findings are constrained by chronological evidence from post-infrared infrared-stimulated luminescence (pIRIR) dating and amino acid geochronology reaching back to >500 ka. Together, the data shed light on Middle to Late Pleistocene depositional and tectonic processes and regional environmental change, and emphasize the significance of the Heidelberg Basin infill as a Quaternary reference profile for Central Europe (cf. Gabriel et al., 2013).

## 2. Regional setting

The Heidelberg Basin, the main depocentre in the distal part of the URG, is infilled by sediments from two distinct sources, one being the eastern graben shoulder, whose highest points overlook the Rhine plain (i.e. the basin's sedimentary fill) by ~500 m, and its hinterland (Gabriel et al., 2013, and references therein). These are the low mountain range of the Odenwald and the southward-adjacent Kraichgau depression, where Triassic sedimentary rocks prevail (Fig. 1), specifically a terrigenous red sandstone of the Early Triassic ('Buntsandstein'), and a grey limestone of the Middle Triassic ('Muschelkalk'; Geyer et al., 2011). This area is drained by the Neckar river that flows into the Rhine plain, and has built up an alluvial fan (Löscher et al., 1980). Additionally, debris from very proximal slopes of the Odenwald finds its way into the Heidelberg Basin via short-distance mass wasting (Ellwanger et al., 2009). The second major source of sediments is the Rhine river system, and notably its Alpine headwaters. These sediments are originally diverse in clast lithologies (Pfiffner, 2010), but mainly quartzitic and crystalline pebbles outlast the long-distance fluvial transport to the Heidelberg Basin (Hoselmann, 2009). This Rhenish sediment input presumably fluctuated considerably throughout the Quaternary due to repeated build-up of extensive and erosive valley glaciers in the Alps (e.g. Ellwanger et al., 2011; Preusser et al., 2011; Schlüchter et al., 2021).

The stratigraphy of unconsolidated deposits in the northern URG and specifically in the Heidelberg Basin has been outlined in detail by Gabriel et al. (2013). The lowermost regional unit is the Iffezheim Formation (Fm.), an intercalation of often intensively weathered reddish- or greyish-white sand and fines derived mainly from the graben shoulders, i.e. the lower mountain ranges (here: Odenwald, Fig. 1) flanking the URG. These deposits have been attributed to the Pliocene by magnetostratigraphy (Scheidt et al., 2015). The overlying Viernheim Fm. Consists of grey fluvial sand and floodplain fines delivered by the Rhine river ('Rhenish facies') in the graben centre, and of little weathered, reddish Neckar-derived sand and gravel as well as lacustrine fines and mass flow deposits at its margin. Here, it can be difficult to distinguish Iffezheim
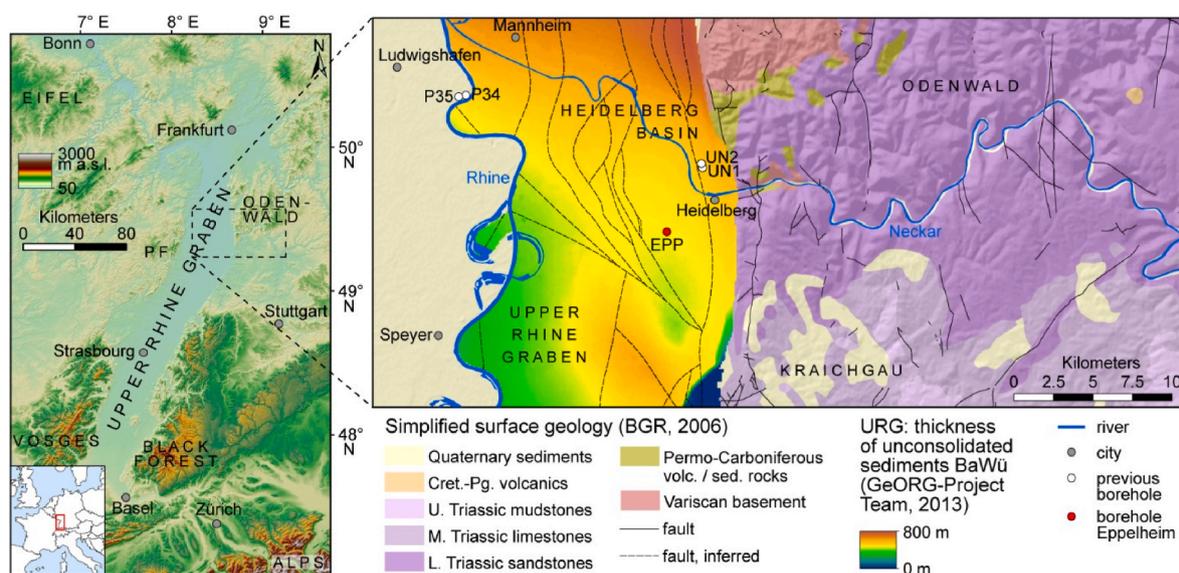


**Fig. 1.** (colour online). Left: Overview map of the Upper Rhine Graben (URG) and surrounding highlands (PF = Palatinate Forest) in Central Europe (BGR, 2006; GeORG-Projektteam, 2013). Right: Vicinity of the EPP drill site (red dot) at the southern margin of the Heidelberg Basin, the URG's main depocenter (cf. thickness of unconsolidated sediments, displayed for the area of Baden-Württemberg state BaWü). P34/P35: boreholes Ludwigshafen-Parkinsel P34/P35, UN1/UN2: boreholes Heidelberg Uni Nord 1/2 (Gabriel et al., 2013, and references therein).

and Viernheim Fm., which stresses the time-transgressive nature of lithostratigraphic boundaries in the URG (cf. Ellwanger et al., 2009). The Rhenish facies reflects the connection of the Upper Rhine to the Alpine headwaters that occurred in the Early Pleistocene (Boenigk, 1982; Hagedorn and Boenigk, 2008; Ziegler and Fraefel, 2009). Thus, the Viernheim Fm. represents the Early Pleistocene as well as part of the Middle Pleistocene (Lauer et al., 2011; Scheidt et al., 2015). A large-scale fining-upward cycle from fluvial sand to silt and clay constitutes the Ludwigshafen Fm. The fines at its top, previously referred to as 'Oberer Zwischenhorizont' ('Upper Intermediate Horizon', referring to its aquitard character), are widespread in the Heidelberg Basin and evidence of a period of regionally high accommodation space-to-sediment supply ratio (Ellwanger et al., 2009). Locally, they are organic-rich or peaty (Wirsing and Luz, 2007). The Ludwigshafen Fm. is of Middle Pleistocene age as evidenced both by presumed Cromerian fossil contents (Knipping, 2008; Wedel, 2009) as well as radiometric dating results (Lauer et al., 2011: infrared-radiofluorescence IR-RF; Li et al., 2018: pIRIR). The Cromerian Complex Stage (Zagwijn, 1985; Head and Gibbard, 2005; here, for simplicity, Cromerian) represents marine oxygen isotope stages (MIS) 21–13 (Böse et al., 2012; i.e. the time period from 866 to 478 ka, MIS boundaries after Lisiecki and Raymo, 2005). However, it remains disputed whether the Ludwigshafen Fm. includes, or terminates before, the Holsteinian Interglacial (cf. Preusser et al., 2021), which was U/Th-dated to MIS 9 in the type area (337–300 ka, Geyh and Müller, 2005) but is widely attributed to MIS 11 (424–374 ka, Kukla, 2003; Lauer and Weiss, 2018; Candy et al., 2024). A sharp increase in grain size marks the transition to the Mannheim Fm., the uppermost stratigraphic unit in the northern URG. Similar to the Viernheim Fm., it consists of Rhine- and Neckar-derived fluvial sediments with some intercalated mass flow diamicts, and very well sorted, fluvially reworked aeolian sands. Frequent facies changes are explained by a combination of fluvial autocyclicity and repeated climate fluctuations (Menzies and Ellwanger, 2015). The deposits of the Mannheim Fm. are attributed to the later Middle and Late Pleistocene as confirmed by different luminescence dating approaches (Lauer et al., 2010: optically stimulated luminescence - OSL; Lauer et al., 2011: IR-RF; Li et al., 2018 and Preusser et al., 2021: OSL and pIRIR).

## 3. Material and methods

### 3.1. Core recovery and initial description

Borehole EPP was drilled in 2021 in the southern part of the town of Eppelheim for groundwater exploration, some 3 km SW of Heidelberg (49.388° N, 8.632° E; Fig. 1), and terminated at a depth of 136 m (31 m b.s.l.). A bucket auger was used to recover the top 24 m of sediments and yielded cores with some disturbance by internal mixing. From 24 to 91 m, cores were recovered protected in plastic liners and in excellent quality, while the interval between 91 and 136 m was drilled destructively and the material was recovered in the shape of fine gravel-sized cuttings. After drilling was completed, a borehole geophysical survey was conducted, including a natural gamma log. The cores and cuttings were photographed, logged, and sampled at the core repository of the Geological Survey of Baden-Württemberg (LGRB).

### 3.2. Gravel petrography

From coarse-grained intervals, nine gravel samples were collected for pebble analysis. These samples consist of the medium to coarse gravel fraction extracted from half or full core intervals by sieving, and comprise between 178 and 527 individual clasts each. The clasts were identified with help of a reference collection at the LGRB, and subdivided into 12 lithology groups (light grey, dark grey, and blackish limestones, red, calcareous, and other sandstones, quartzites, vein quartzes and cherts, granites, gneisses, and volcanic rocks). The petrographic compositions of the gravel samples were evaluated by

correlation as well as principal component analysis using the freeware program Past 4 (Hammer et al., 2001). For the three most abundant lithologies, light and dark grey limestones and red sandstones, the clast rounding was determined after Powers (1953; six classes from very angular to well rounded). Where otherwise rounded clasts had sharp, freshly broken edges, these were regarded as drilling artefacts and discarded.

### 3.3. Grain size analysis

Grain size analysis of fine-grained intervals was performed at a 10-cm-resolution by laser diffraction spectroscopy using a Malvern Panalytical Mastersizer 3000 at the University of Freiburg, and following the standard operating protocol by Abdulkarim et al. (2021). Samples comprising 5–15 g of material sieved to <1 mm in order to prevent clogging of the system were treated first for 12 h with 15% $H_2O_2$ in order to remove organic material, and then another 12 h with Calgon (33 g sodium hexametaphosphate and 7 g sodium carbonate in 1 l of water) in order to disaggregate cohesive grains. Each data point consists of the average of five subsample measurements where the particle size distributions were calculated using the Mie theory (Wriedt, 2012). This approach is fast and reproducible but has been shown to consistently underestimate clay contents, and therefore we complied with the in-house standard procedure of shifting the clay-silt boundary to 6.3 μm (cf. Schulze et al., 2022; Schwahn et al., 2023).

### 3.4. Loss-on-ignition

Carbonate and total organic carbon (TOC) contents in selected intervals were determined by the loss-on-ignition approach (LOI; Heiri et al., 2001). Samples of 1–4 g of sediment were oven-dried, crushed and heated to 550 °C in a furnace, and TOC determined from the resulting mass loss ($LOI_{550}$) by (1) (Heiri et al., 2001; Vereș, 2002).

$$TOC = \left( \frac{LOI_{550}}{dry\ sample\ mass} \right) * 0.5 \qquad (1)$$

In a second step, the samples were heated to 950 °C, resulting in calcination of carbonates. Assuming that all carbonate occurs as $CaCO_3$, its content $X(CaCO_3)$ can be calculated from the mass loss ($LOI_{950}$) as (2) (Heiri et al., 2001).

$$X(CaCO_3) = \left( \frac{LOI_{950}}{dry\ sample\ mass} \right) * 2.27 \qquad (2)$$

### 3.5. Palynological analysis

From the lower fossiliferous interval, we selected a total of 38 samples of ~1 cm³ of sediment each for pollen analysis. These consist of one sample every 10 cm from 55.1 to 58.1 m, and two samples every metre from 58.1 to 63.5 m. The sample preparation followed Faegri and Iversen (1989). All samples were decalcified with 10 % HCl, spiked with *Lycopodium* spores, and cooked in 10 % KOH. Sieved to <0.3 mm, palynomorphs were separated from sediment grains by density separation using sodium polytungstate (which has been shown to be as effective as chemical treatment, e.g. with potentially hazardous hydroflouric acid; Campbell et al., 2016; Leipe et al., 2019) and, after acetolysis with acetic anhydride and $H_2SO_4$, fixed in glycerine. Pollen grains were identified at 400x and 1000x magnification using the pollen key to Beug (2004) and a reference collection. For the calculation of pollen percentages, Cyperaceae, aquatics and spores were excluded. Pollen nomenclature follows Beug (2004), and spores are named according to Reille (1998).

### 3.6. Macrofossil identification

Intact, mm-sized fossil shells were encountered during initial core logging in two intervals at 24–26 and 54–64 m depth. The respective drill cores were thus subdivided into 10-cm-thick samples (92 in total) which were left to soak and disintegrate in water for 12 h, and then wet-sieved using several mesh sizes from 8 to 0.25 mm to facilitate separating small shells from partly abundant plant fragments. Fossils, mainly gastropod shells, were hand-picked from the sieves with a needle and a fine wet brush, and identified under a binocular microscope. The taxonomy follows the latest updates of Bank et al. (2014: www.mollusc abase.org, last accessed 18.12.2023), and ecological grouping of identified taxa follows Ložek (1964), Puisségur (1976), and Rähle (2005). Minimum numbers of individuals have been estimated according to Ložek (1964). Often preferentially accumulated (Gilbertson and Hawkins, 1978) and/or preserved (Marcussen, 1967) and thus over-represented, opercula have only been used for counting in absence of shells or shell fragments of their respective taxa.

### 3.7. Amino acid dating

Eleven individual gastropod opercula from three selected layers (55.3–55.4 m depth: 3x *Parafossarulus crassitesta*; 56.7–56.8 m and 58.7–58.8 m: 4x *Bithynia tentaculata* each) were picked for amino acid analysis using the intra-crystalline protein decomposition approach (IcPD) as an additional geochronological tool (Penkman et al., 2011). In brief, following the methods of Penkman et al. (2008), the intra-crystalline protein from individual powdered opercula was isolated by bleaching with NaOCl. Then, two subsamples were taken from each bleached operculum. The first subsample was demineralised and the naturally occurring free amino acids (FAA) analysed. The second subsample was treated with 7 M HCl and heated at 110 °C for 24 h to release the peptide-bound amino acids, yielding the 'total hydrolysable amino acid' fraction (THAA). Each subsample was analysed in duplicate by reverse-phase high-pressure liquid chromatography (Kaufman and Manley, 1998), along with standards and blanks.

During preparative hydrolysis rapid irreversible deamination of asparagine and glutamine to aspartic acid and glutamic acid, respectively, occurs (Hill, 1965). As such these two pairs of amino acids are reported together as Asx and Glx. The concentrations and D/L values of aspartic acid/asparagine, glutamic acid/glutamine, alanine, and valine (D/L Asx, Glx, Ala, Val) are assessed to provide an overall estimate of intra-crystalline protein decomposition. In a closed system (e.g. within an unaltered biomineral), the amino acid ratios of the FAA and the THAA subsamples should be highly correlated, enabling the recognition of compromised samples (Preece and Penkman, 2005). Each amino acid racemises (i.e. increases in D/L value) at a different rate, which provides age discrimination over different timescales from several thousand to several hundred of thousand years. In bithyniid opercula, the rate of racemisation varies from fastest to slowest in the following order: Asx > Ala > Glx > Val (Penkman et al., 2013).

### 3.8. Luminescence dating

We collected eleven samples for luminescence dating from seemingly undisturbed, ideally well-sorted, sand-dominated intervals between 10 and 85 m depth. Sampling was done at night time under subdued red light, and each sample comprises material from a ~20 cm section. The upper 2–3 cm of sediment at the core surface were stripped off and saved for gamma spectroscopy, and the material below was collected in opaque bags. For gamma spectroscopy, the respective samples were sieved to <2 mm. The sample at 29.3 m depth was notably coarser than the remaining samples and was therefore crushed in a jaw crusher beforehand. All gamma samples were then filled into plastic containers and measured using an Ortec High Purity Germanium gamma spectrometer at University of Freiburg (details in Preusser et al., 2023). For dose rate

determination we used the ADELEv2017 software (Degering and Degering, 2020; www.add-ideas.com, last accessed 25.12.2023), assuming an alpha efficiency (a-value) of $0.07 \pm 0.02$ and an average water content of $20 \pm 10$ %.

In the red-light laboratory at the University of Freiburg, the luminescence samples were sieved to 200–250 µm, carbonates were removed with 20% HCl, and K-feldspar was separated from quartz and heavy minerals using a heavy liquid ($\delta = 2.58$ g cm$^{-3}$). Part of the K-feldspar separates were mounted on stainless steel discs with a diameter of 1 mm coated with silicon oil as adhesive. Luminescence measurements were carried out on a Freiberg Instruments *Lexsyg Smart* device (Richter et al., 2015). A 3-mm-thick Schott BG 39 glass filter in combination with a 414/46 AHF Brightline interference filter was used to narrow transmission window to the main luminescence emission of K-feldspar (410 nm). The beta source in the machine was calibrated using the Lex-Cal2014 quartz (Richter et al., 2020) to ca. 0.62 Gy s$^{-1}$ on stainless steel discs (this particular device is equipped with a much stronger $^{90}$Sr/$^{90}$Y source than most other machines). A modified version of the Single Aliquot Regenerative (SAR) dose Multi-Elevated Temperature (MET) pIRIR protocol after Li and Li (2011) with five irradiation cycles including zero dose and recycling was used for determination of the equivalent dose ($D_e$). Compared to the original protocol, the preheat temperature was reduced to 230 °C and the stimulation step at 250 °C was omitted (Table 1). This was done as the effective temperature at the sample carrier discs varies significantly between the different types of readers (Schmidt et al., 2018), compared to the temperature reported by the manufacturer. While the so-called 110 °C TL peak of quartz typically observed on Risø readers is at ca. 90 °C on most *Lexsyg* devices, the offset appears to become more pronounced at temperatures above 150 °C (Mueller et al., 2020). Temperatures above 250 °C can result in massive changes in sample sensitivity, which may result in producing incorrect data (Chen et al., 2013; Preusser et al., 2021). Performance tests on the applied protocol resulted in dose recovery ratios within 10 % of unity and negligible thermal transfer. Fitting of growth curves was done using the sum of two exponential functions, which provided a much better fit than using a single exponential function.

## 4. Results

### 4.1. Sediment sequence

The Quaternary succession of the EPP sequence starts with several decametres of sand and gravel (136.0–87.4 m depth, Fig. 2) that are attributed to the Viernheim Fm. It comprises sandy gravel to gravelly sand including some silty-diamictic interbeds (Fig. 2). This section has been recovered mainly by destructive rotary drilling, obliterating finer (sub-metre) structures, but it can be subdivided into a fining-, followed by a coarsening-upward sequence (136.0–112.9 and 112.9–87.4 m, respectively), with a gamma signal peak of ~50 API in between. Clast fragments consist predominantly of red sandstone and grey limestones that crop out in large parts of the Neckar catchment (Lower Triassic

**Table 1**
Overview of the SAR MET pIRIR protocol used in this study.

| Step | Operation | Measurement |
|---|---|---|
| 1 | Give dose, $D_i$ (not in first cycle) | – |
| 2 | Preheat at 220 °C for 60 s | – |
| 3 | IR stimulation at 50 °C for 120 s | $L_x$ (50 °C) |
| 4 | IR stimulation at 100 °C for 120 s | $L_x$ (100 °C) |
| 5 | IR stimulation at 150 °C for 120 s | $L_x$ (150 °C) |
| 6 | IR stimulation at 200 °C for 120 s | $L_x$ (200 °C) |
| 7 | Give test dose, $D_t$ (~54 Gy for most samples) | – |
| 8 | IR stimulation at 50 °C for 120 s | $T_x$ (50 °C) |
| 9 | IR stimulation at 100 °C for 120 s | $T_x$ (100 °C) |
| 10 | IR stimulation at 150 °C for 120 s | $T_x$ (150 °C) |
| 11 | IR stimulation at 200 °C for 120 s | $T_x$ (200 °C) |
| 12 | Return to step 1 | – |
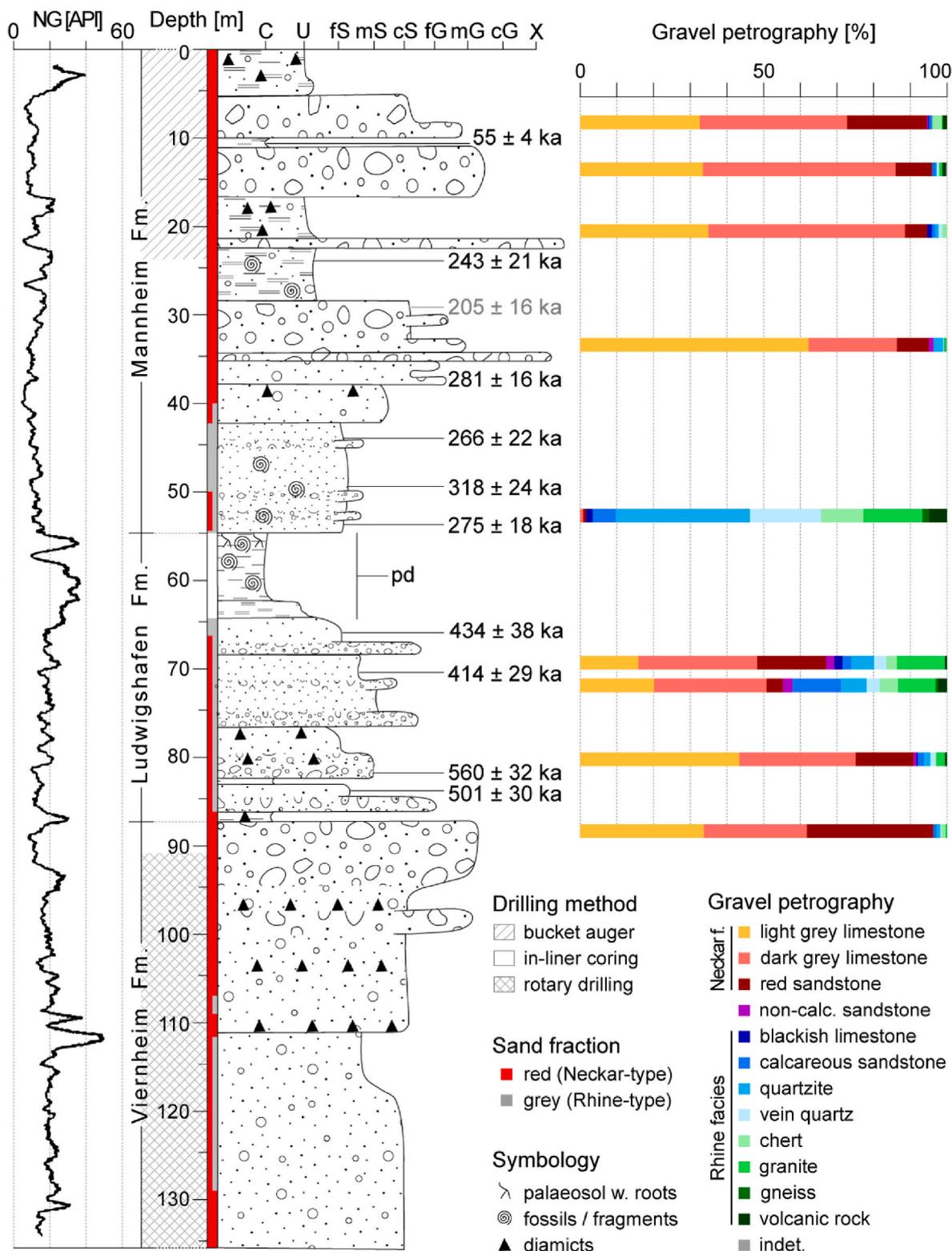
**Fig. 2.** (colour online). Sedimentological profile of borehole EPP, including natural gamma log (NG), luminescence ages (MET pIRIR-200) and petrographic characterisation of the gravel and sand fractions (see section 'Sediment provenance'). C = clay, U = silt, S = sand, G = gravel, X = cobbles, f = fine, m = medium, c = coarse. pd = palustrine deposits with bio- and aminostratigraphic constraints.

'Buntsandstein' and Middle Triassic 'Muschelkalk'). Above 91 m depth, where the sediment is better preserved due to in-liner coring, clasts up to cobble size occur as well as mud balls, i.e. rip-up clasts consisting of fine and cohesive but unconsolidated material. Sandstone pebbles are frequently angular to subrounded, whereas the limestones are mostly rounded. Two endmembers are identified in the sand fraction and occur both as pure intervals or as a mixture. The first sand type is medium-to coarse-sized, rather angular in grain shape, and reddish in colour, and is delivered by the Neckar river. The second type is greenish-grey, and consists of more rounded and notably finer grains, including some

carbonaceous material as well as muscovite flakes. This sand type is attributed to the Rhine river, and is restricted to the interval from 128.9 to 108.0 m, whereas the Neckar sand occurs throughout the entire first section.

Further up the succession, the deposits become progressively finer, characteristic of the Ludwigshafen Fm (87.4–55.0 m). This is associated with an increase in the gamma signal from ~10 API at the bottom to ~40 API at the top. From 87.4 to 69.2 m, several metre-scale fining-upward cycles consist of rather fine, well-sorted sand with only minimal silt (Fig. Fig. 2). Diamictic interbeds of gravelly silt occur at ~87, ~80 and ~78 m depth. Gravel beds in this section are more diverse in composition, comprising rounded pebbles of greyish sandstone, quartzite, and crystalline rocks, as well as the previous sand- and limestones. The sand fraction is mostly a mixture of both aforementioned red and grey sand types. Silt occurs in the shape of well-sorted, yellow-beige decimetre-interbeds, sometimes with metal oxide crusts, and individual mud balls. A large-scale fining-upward cycle extends from 69.2 to 55.0 m. It begins with a sandy gravel in which grey limestone and red sandstone are gradually replaced by well-rounded quartzite and granite clasts, and which grades into pure green-grey sand with faint, mm-to cm-scale bedding. Fines start to dominate at ~65 m, with laminated yellow-beige silt transitioning into grey, partly brownish, massive silty clay. In this interval, frequent shells and shell fragments of small (few mm) gastropods occur as well as mm-to cm-sized, partly coaly, wood fragments.

At 55.0 m, the fines are sharply truncated and replaced by a diverse succession of sand, gravel and diamict (Mannheim Fm.; Fig. 2). From 55.0 to 42.8 m, fine greenish-grey sand dominates, with some admixtures of reddish sand. Some layers contain fine-medium gravel clasts of diverse lithologies, and isolated shell fragments occur throughout the section. Coarse reddish sand alternates with subangular to rounded sandy gravels consisting of red sandstone and grey limestone from 42.8 to 28.0 m, while no fine greenish-grey sand occurs above 40 m depth. A clast-supported diamictic interbed from 36.9 to 36.0 m comprises subangular, mainly fine-medium gravels in a poorly sorted, sandy to clayey matrix, and is overlain by 1.3 m of cobbles. At 28.0 m, the material changes abruptly to a massive silt of brown and later yellowish colour that contains dispersed gastropod shells, and a gravelly-diamictic interbed at 27.6–27.4 m. The cores above 24 m depth allow for less detailed descriptions. Above a coarse interbed of gravel and cobbles from 22.8 to 21.7 m, a diamict of red sandstone and grey limestone clasts in a brownish silty and, at the bottom, sandy matrix continues to 17.3 m depth. It is overlain by 6 m of sandy gravel with cobbles comprising few quartzites and granites but mostly the aforementioned sand- and limestones. Several diamictic packages follow, starting with yellowish-grey silt at 11.5–10.3 m, followed by a reddish, gravelly fining-upward cycle with mud balls until 6.4 m, and brownish gravelly-sandy silts with anthropogenic debris near the ground surface.

## 4.2. Palustrine deposits in detail

The interval from 64.0 to 55.0 m depth comprises silty to clayey fine sediments with abundant macrofossils and was analysed in greater detail. It consists of three fining-, followed by one coarsening-upward cycle (Fig. 3). The first cycle (F1, 64.0–61.0 m) starts with an initially laminated but mostly massive, ochre-beige sandy silt with ~25 % of $CaCO_3$ grading into a brownish-grey silty clay. Above 63.0 m, TOC increases from <1 % to ~2 %, with higher values coinciding with a distinct smell of $H_2S$, and gastropod shells start to occur. In the following cycle, brownish-grey clayey silt (F2a, 61.0–59.3 m) is overlain by grey silty clay with oxidised-red stains (F2b, 59.3–58.5 m). The latter contains first, partly coaly, wood fragments and, from 59.0 to 58.5 m, Characeae oogonia. The third cycle starts with an abrupt increase in $CaCO_3$ content to ~50 %, associated with a drop in TOC to ~1 %. Both values remain approximately constant for 1.5 m (F3a, 58.5–57.0 m). This interval is mainly silt-sized and reddish-beige, and shows a distinct drop in the natural gamma signal (Fig. 2). Above (F3b, 57.0–56.6 m), the carbonate content declines to <10 %, while TOC starts to increase again. This trend in TOC, with maximum values of ~5 %, continues throughout the final coarsening-upward cycle (C, 56.6–55.0 m) consisting of grey
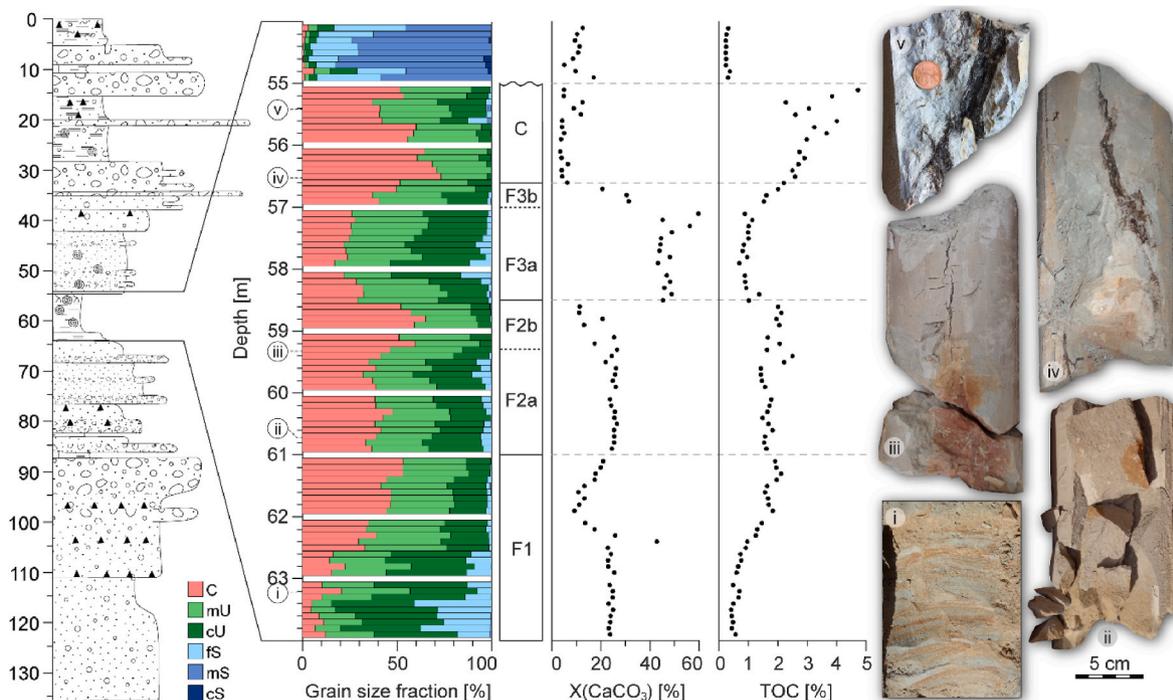


**Fig. 3.** (colour online). Grain size and composition data of the interval from 64.0 to 54.0 m depth, consisting of three fining- (F1-F3), and one coarsening-upward cycle (C) truncated at 55.0 m. On the right, selected core photos are presented: i – loose laminated sandy silt at 63.3 m, ii – beige clayey silt at 60.8 m, iii – grey clayey silt with oxidised reddish stains at 59.4 m, iv and v – silt and clay with wood fragments, likely tree roots, at 56.6 and 55.5 m, respectively. C = clay, U = silt, S = sand, f = fine, m = medium, c = coarse.

silty clay with generally <10 % CaCO$_3$. Here, larger dark brown wood fragments occur, including vertical strands, likely tree roots, of 2–3 cm diameter and several decimetres length. Apart from the top ~50 cm, gastropod fossils are entirely lacking in this final cycle. The succession of fines is sharply truncated by an ochre-beige, slightly gravelly sand at 55.0 m (Fig. 3).

### 4.3. Pollen assemblages

Seven local pollen zones (LPZ) could be identified in the interval from 62.1 to 55.1 m depth (Fig. 4). While the lowermost two samples (63.5 and 62.5 m) contained no pollen, the following three samples representing LPZ 1 (62.1–60.8 m) are characterised by relatively low arboreal percentages (mainly *Pinus* and *Betula*), and the herbal pollen spectrum is dominated by Poaceae and *Artemisia*. In the uppermost sample the frequent occurrence of *Thalictrum* is noteworthy. LPZ 2 (60.8–58.8 m) shows increasing arboreal proportions (up to 70 %). In the lower part of the pollen zone the arboreal content is mainly composed of *Pinus*, whereas in the upper part, *Betula* is more important. The non-arboreal pollen spectrum is still dominated by Poaceae, *Artemisia*, and *Thalictrum*. LPZ 3 (58.8–58.1 m) is characterised by a decrease in arboreal pollen to around 40 %, accompanied by more frequent occurrence of heliophytes (e.g. *Artemisia*, *Thalictrum*, *Helianthemum*, and Chenopodiaceae) and other taxa typical of open conditions, like *Juniperus*, *Selaginella*, and *Botrychium*.

LPZ 4 (57.8–57.6 m) shows 80–90 % of arboreal taxa, especially *Alnus*, *Pinus*, *Quercus*, and *Ulmus*. *Corylus* is present with values around 7% and *Picea* with proportions around 3%. The pollen content of LPZ 5 (57.4–57.15 m) encompasses co-dominance of *Pinus* and *Alnus*. Besides that, thermophilous deciduous trees, such as *Quercus*, *Ulmus*, *Carpinus*, and *Corylus*, reach values around 30 %. LPZ 6 (57.15–56.75 m) is characterised by increasing *Alnus* (up to 40%) and decreasing *Pinus* and thermophilous deciduous tree values. LPZ 7 (56.75–55.1 m) consists of 16 samples with total arboreal pollen contents of >80%. *Alnus* (20–50 %) is accompanied by *Abies* (15–25 %) and a low presence of thermophilous trees, such as *Quercus*, *Ulmus*, *Carpinus*, and *Fagus*. Noteworthy is also the occurrence of *Buxus*. Furthermore, there is a high presence of *Azolla filiculoides* (especially in the upper part of the pollen zone) with up to 121 % of the reference sum. Apart from *Azolla*, further aquatic taxa such as *Polygonum persicaria*-type, *Potamogeton*, *Myriophyllum*, *Nuphar*, *Nymphaea*, and *Trapa*, as well as glochidia-bearing massulae of *Azolla filiculoides* are characteristic of LPZ 7.

### 4.4. Mollusc assemblages

In total, 92 sediment samples were sieved for macrofossils, nine of which were sterile or contained only small shell fragments that could not be identified. More than half of the samples contain ≤10 individuals and only about 15 % exceed 30 individuals, with a maximum number of 61 at 58.6–58.7 m depth. The maximum number of taxa is 19 at 62.1–62.2 m. Seven local mollusc zones (LMZ) were identified from 62.9 to 54.0 m, and one LMZ from 25.5 to 24.2 m depth (Fig. 5). In the lower interval, most LMZ include both terrestrial and aquatic taxa, whereas the upper interval contains almost exclusively terrestrial species.

With 21 taxa, LMZ 1 (62.9–61.3 m) is remarkably diverse and contains both terrestrial (e.g. *Arianata arbustorum*, *Vallonia* sp., *Succinea putris*) as well as aquatic species (e.g. *Bithynia* sp., *Anisus* sp., *Valvata piscinalis*). Following a peak in both abundance and diversity of molluscs at ~62 m, the assemblage becomes dominantly terrestrial. This terrestrial signal continues into LMZ 2 (61.3–60.9 m) which is characterised by the only occurrences of *Pupilla alpicola* and *Vallonia tenuilabris*, and into LMZ 3 (60.8–59.6 m), where *Perforatella bidentata*, missing in LMZ 2, reappears. Generally, LMZ 3 is however rather poor in both number and diversity of molluscs. A drastic change marks the onset of LMZ 4 (59.5–58.4 m). Here, the molluscan fauna is almost exclusively aquatic and presents a relatively high diversity of seven or more species in most

samples (e.g. *Bithynia* sp., *Anisus spirorbis*, *Stagnicola palustris*). At 59.4–58.9 m, *Euglesa nitida*, *Pisidium amnicum*, as well as small rounded nacreous fragments of other mussels occur. Above 59.0 m, opercula of *Bithynia tentaculata* occur abundantly, almost an order of magnitude more frequently than the corresponding shells. Oogonia of Characeae are also characteristic for this interval.

Terrestrial taxa such as *Cepaea* sp. and *Carychium minimum* reappear only in LMZ 5 (58.2–56.6 m), and increase notably in abundance and diversity at ~57 m (e.g. *Vitrea crystallina*, *Perforatella bidentata Oxychilus* cf. *Cellarius*. After an entirely sterile interval from 56.6 to 55.6 m, LMZ 6 (55.6–55.1 m) is again characterised almost exclusively by aquatic species occurring in relatively low numbers (*Anisus* sp., *Gyraulus crista*, *Valvata* spp.). Separated by a sharp facies boundary (see Fig. 3), LMZ 7 (55.0–54.0 m) has a sparse mollusc assemblage of mostly terrestrial species occurring in low numbers and generally poorly preserved, with worn shell surfaces, holes, and brown-reddish incrustations. Finally, LMZ 8 occurs significantly further up in the succession (25.5–24.2 m) and comprises mainly terrestrial taxa. The dominant species are *Trochulus hispidus* and *Vallonia costata*.

### 4.5. Amino acid racemisation

IcPD in eleven opercula of the two bithyniid taxa *Bithynia tentaculata* and *Parafossarulus crassitesta* were analysed. Both FAA and THAA are well correlated (Fig. 6), which demonstrates a closed system has been retained in all samples analysed. Fig. 6 further shows the THAA D/L values of aspartic acid/asparagine (Asx; ~0.8), alanine (Ala; ~0.7), glutamic acid/glutamine (Glx; ~0.5), and valine (Val; ~0.4). In general, the average D/L value increases slightly with depth, consistent with the stratigraphy. The fast racemising Asx is an exception; the D/L values from this amino acid are approaching racemic equilibrium, at which point the natural variability within the data prohibits any further age discrimination.

### 4.6. Luminescence results

The results of dose rate determination are summarised in Table 2. The MET protocol results in four estimates of D$_e$, which reflect the amount of radiation absorbed since the time of burial. However, the D$_e$ determined increases with stimulation temperature, mainly due to the fact that part of the pIRIR signal stimulated at lower temperatures is unstable (cf. Li and Li, 2011). As a result, we will concentrate on the pIRIR signal stimulated at 200 °C in the presentation and discussion (cf. Schwahn et al., 2023).

No samples could be taken from the lower part of the sequence (Viernheim Fm.), due to the destructive drilling technique applied there. For the bottom of the Ludwigshafen Fm., two ages of 501 ± 30 ka (EPP-1: 84.4–84.6 m) and 560 ± 32 ka (EPP-2: 82.4–82.6 m) overlap narrowly within uncertainties. The next two samples from the middle part of the same formation date to 414 ± 29 ka. (EPP-3: 73.4–73.6 m) and 434 ± 38 ka (EPP-4: 67.1–67.3 m). For the lower part of the Mannheim Fm., four ages (EPP-5 to −8) agree well and indicate rapid deposition at ~290 ka, while samples EPP-9 (205 ± 16 ka) and EPP-10 (243 ± 21 ka) from its middle part are just outside the 1-sigma standard deviations. An age of 55 ± 4 ka was determined for the upper part of the Mannheim Fm. (Table 2).

## 5. Discussion

### 5.1. Sediment succession

#### 5.1.1. General lithostratigraphy

The Viernheim Fm (136.0–87.4 m depth; Gabriel et al., 2013, and references therein). is poorly recovered due to destructive rotary drilling below 91 m, but appears to be mostly uniform without larger sedimentological changes. It is of predominantly fluvial origin, with the
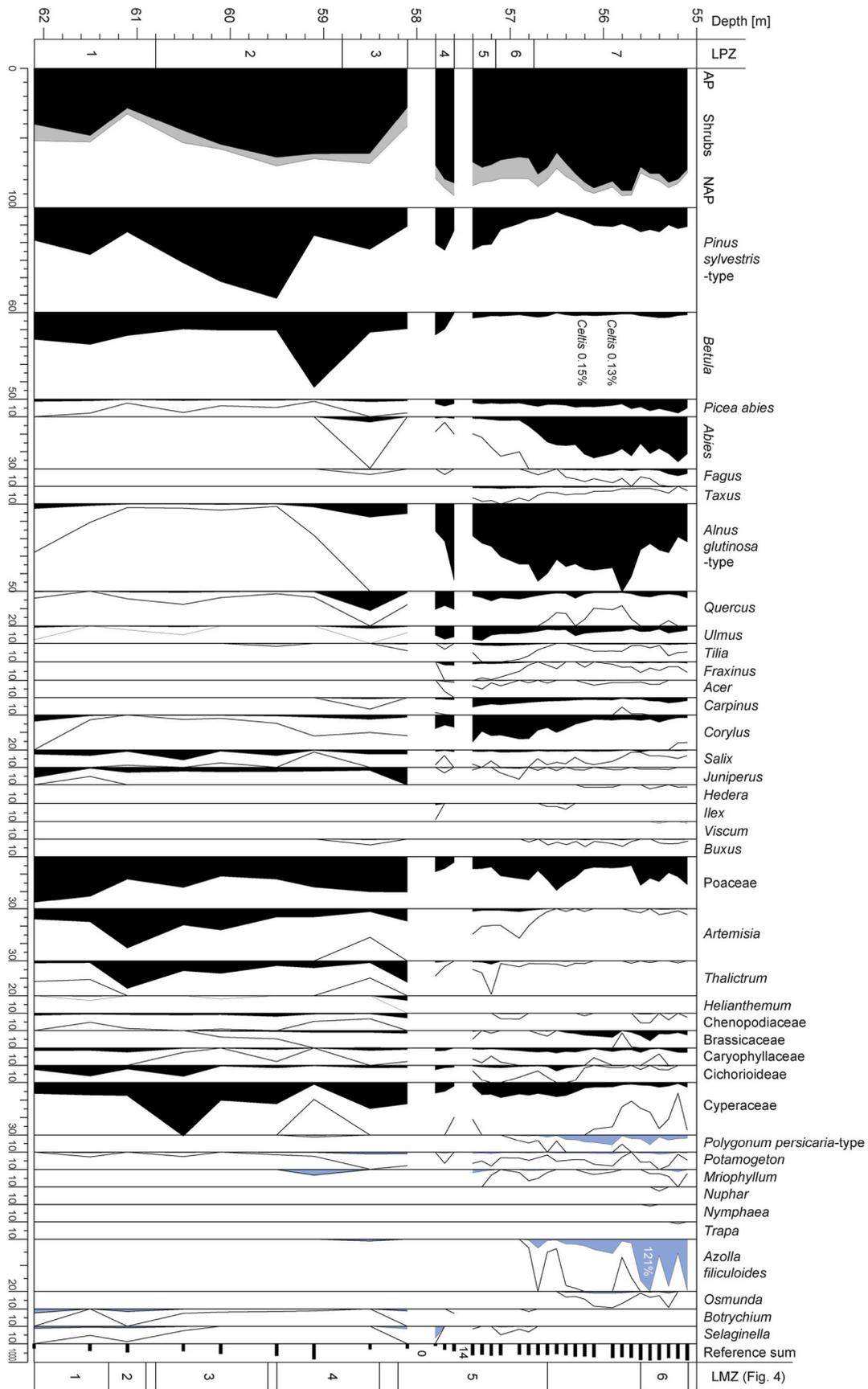
**Fig. 4.** (colour online). Pollen assemblages and local pollen zones (LPZ) of the palustrine interval at 62-55 m depth in EPP. Aquatic taxa are displayed in blue.
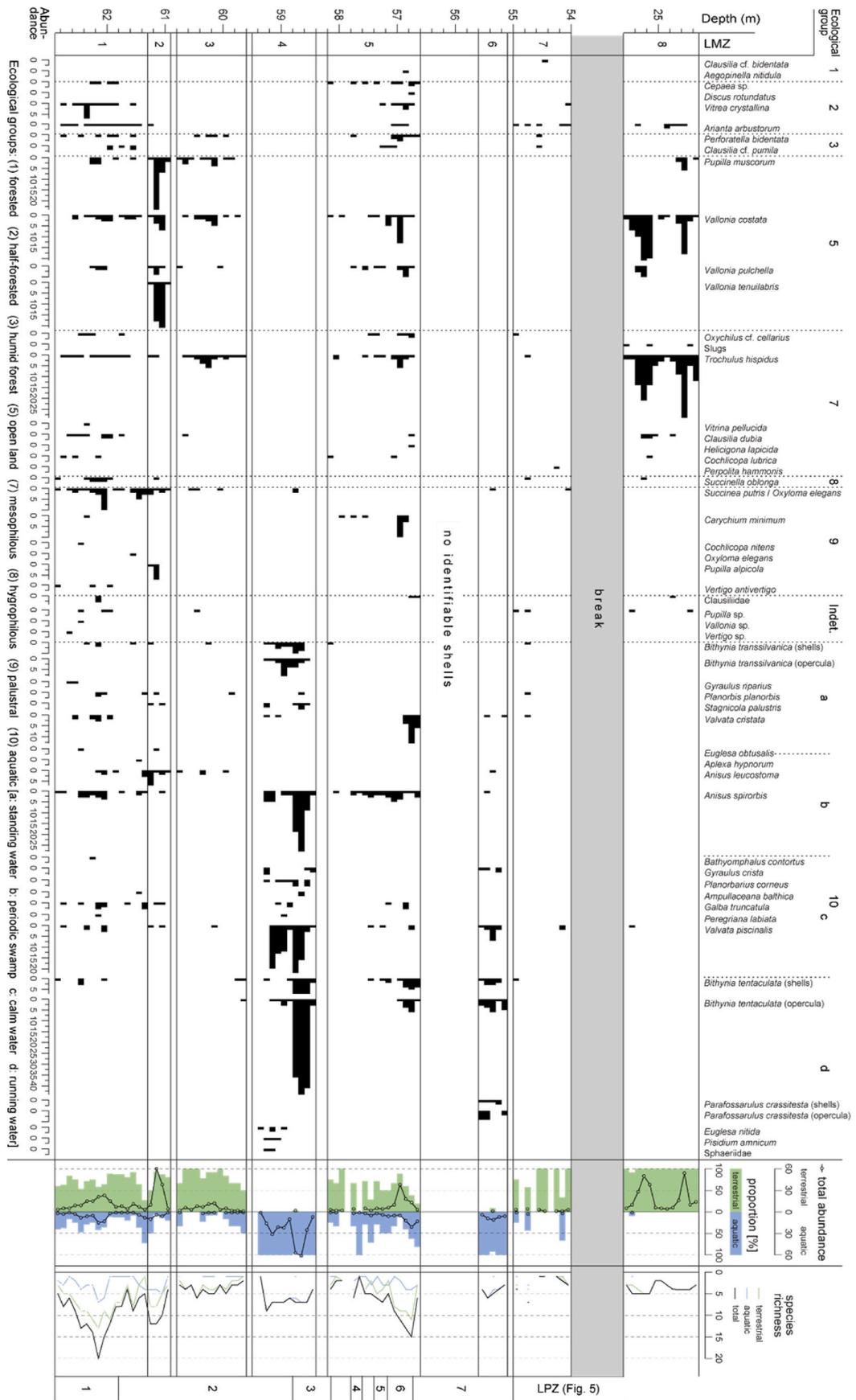
**Fig. 5.** (colour online). Mollusc assemblages and local mollusc zones (LMZ) of fine-grained intervals in EPP.
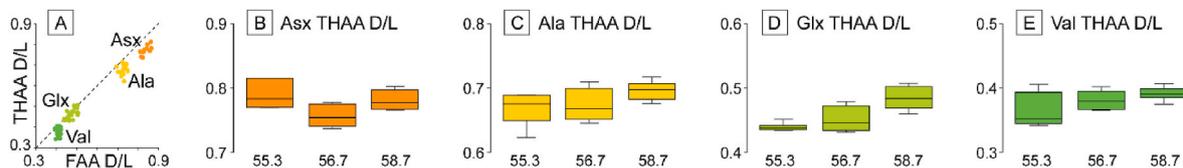
**Fig. 6.** (colour online). A) FAA vs. THAA D/L values of aspartic acid/asparagine (Asx), alanine (Ala), glutamic acid/glutamine (Glx), and valine (Val) for bithyniid opercula from Eppelheim. B)-E) Comparison of the THAA D/L values from three horizons at 55.3 (*P. crassitesta*), 56.7, and 58.7 m depth (both *B. tentaculata*).

**Table 2**
Summary data of pIRIR dating with the position of the sample below surface (depth), the concentration of dose-rate relevant elements (K, Th, U), the resulting dose rate (D), as well as $D_e$ determined for different stimulation temperatures and the resulting pIRIR age for stimulation at 200 °C (Lexsyg).

| Sample | Depth (m) | K (%) | Th (ppm) | U (ppm) | D (Gy. ka$^{-1}$) | $D_e$ IR-50 (Gy) | $D_e$ pIR-100 (Gy) | $D_e$ pIR-150 (Gy) | $D_e$ pIR-200 (Gy) | Age pIR-200 (ka) |
|---|---|---|---|---|---|---|---|---|---|---|
| EPP-12 | 10.7–11.0 | 1.69 ± 0.05 | 7.78 ± 0.51 | 2.43 ± 0.16 | 3.31 ± 0.26 | 105.9 ± 6.9 | 143.5 ± 8.7 | 167.7 ± 10.3 | 183.1 ± 11.4 | 55 ± 4 |
| EPP-10 | 24.0–24.3 | 1.65 ± 0.04 | 10.08 ± 0.64 | 2.50 ± 0.14 | 3.40 ± 0.29 | 501.4 ± 9.4 | 613.9 ± 12.7 | 613.9 ± 12.7 | 827.4 ± 31.0 | 243 ± 21 |
| EPP-9 | 29.2–29.4 | 0.77 ± 0.02 | 1.98 ± 0.23 | 0.62 ± 0.05 | 1.85 ± 0.15 | 232.8 ± 4.2 | 299.5 ± 5.7 | 345.9 ± 7.2 | 380.0 ± 24.6 | 205 ± 16 |
| EPP-8 | 37.4–37.6 | 0.81 ± 0.02 | 1.97 ± 0.21 | 0.57 ± 0.05 | 1.87 ± 0.10 | 315.9 ± 26.5 | 409.4 ± 15.1 | 474.0 ± 17.5 | 525.4 ± 16.7 | 281 ± 16 |
| EPP-7 | 44.4–44.6 | 1.39 ± 0.04 | 4.95 ± 0.31 | 1.06 ± 0.06 | 2.58 ± 0.22 | 503.4 ± 36.9 | 541.3 ± 32.2 | 629.6 ± 38.6 | 686.6 ± 47.3 | 266 ± 22 |
| EPP-6 | 49.4–49.6 | 1.65 ± 0.04 | 3.52 ± 0.28 | 0.84 ± 0.06 | 2.65 ± 0.20 | 605.3 ± 18.4 | 690.8 ± 22.6 | 793.2 ± 29.5 | 845.0 ± 45.1 | 318 ± 24 |
| EPP-5 | 54.4–54.6 | 1.46 ± 0.04 | 3.93 ± 0.31 | 0.90 ± 0.07 | 2.54 ± 0.17 | 470.5 ± 74.3 | 529.2 ± 38.6 | 636.4 ± 30.6 | 699.9 ± 29.3 | 275 ± 18 |
| EPP-4 | 67.1–67.3 | 1.52 ± 0.04 | 4.94 ± 0.36 | 1.09 ± 0.06 | 2.49 ± 0.22 | 644.4 ± 59.6 | 822.2 ± 53.0 | 1014.7 ± 58.1 | 1079.4 ± 76.7 | 434 ± 38 |
| EPP-3 | 73.4–73.6 | 1.59 ± 0.04 | 3.53 ± 0.28 | 0.97 ± 0.07 | 2.43 ± 0.17 | 621.6 ± 43.4 | 861.3 ± 19.1 | 997.7 ± 25.4 | 1099.9 ± 42.7 | 414 ± 29 |
| EPP-2 | 82.4–82.6 | 0.60 ± 0.02 | 1.79 ± 0.20 | 0.54 ± 0.03 | 1.48 ± 0.10 | 391.6 ± 14.0 | 632.2 ± 20.1 | 750.4 ± 19.9 | 829.7 ± 25.0 | 560 ± 32 |
| EPP-1 | 84.4–84.6 | 0.93 ± 0.03 | 2.26 ± 0.26 | 0.62 ± 0.05 | 1.78 ± 0.11 | 497.7 ± 9.0 | 666.5 ± 19.4 | 793.7 ± 19.7 | 892.0 ± 27.6 | 501 ± 30 |

silty-diamictic interbeds pointing towards episodes of colluvial input, for example by debris flows, and likely under rather cold, peri-glacialconditions (e.g. Menzies and Ellwanger, 2015; Preusser et al., 2021). Mud balls within gravel layers at the top of the interval are indicators of recurring flooding events (Karcz, 1969; Bachmann and Wang, 2014). Notable fine-grained, potentially lacustrine sections (cf. Gabriel et al., 2013) could not be identified with certainty in the present record, although peaks in the gamma log at ~110 m depth indicate an abundance of clay minerals. These peaks may alternatively indicate phases of intense weathering.

The Ludwigshafen Fm (87.4–55.0 m; Gabriel et al., 2013, and references therein). consists of a large-scale fining-upward cycle that begins with graded packages of fluvial, partly gravelly sand that indicate generally lower flow velocities than during deposition of the Viernheim Fm. Interbedded layers of silt are interpreted as floodplain deposits, and diamictic layers might point toward crevasse splays associated with flood events (Przyrowski and Schäfer, 2015). The fluvial gravel and sand grade into a succession of silt and clay from 64.0 to 55.0 m depth (Fig. 3). It represents a palustrine environment with local variations in sediment input over time, as indicated by metre-scale internal packages. This would be expected in a floodbasin fed by recurring overbank flow spills. For example, the interval from 58.5 to 57.0 m depth is enriched in carbonatic material that notably dilutes the TOC content (Fig. 3), although pedogenic precipitation of carbonate might have played a role, too. Generally, the initially low but increasing TOC content, as well as increasing amounts in plant fragments and, later, intact tree roots are indicative of initially cool but steadily ameliorating climate conditions (which is supported by floral and faunal remains, see below) terminating in a palaeosol.

Following a sharp and potentially erosive boundary, diverse fluvial-

dominated deposits constitute the Mannheim Fm. from 55.0 m depth to the surface (Ellwanger et al., 2009; Gabriel et al., 2013). The character of these sediments changes frequently, including well-sorted sand and gravel, block layers, diamictic colluvial interbeds as well as fines-dominated packages (Fig. 2). Menzies and Ellwanger (2015) explained these variations by a combination of fluvial autocyclicity, i.e. a varying distance from one or more laterally migrating channels, and of recurring cold and warm climatic periods and associated geomorphic processes (e.g. mass movements and soil formation, respectively).

*5.1.2. The palustrine deposits conundrum*

The palustrine deposits at the top of the Ludwigshafen Fm. are a regionally widespread, typically 10–20 m (at Heidelberg Uni Nord the entire 70-m-thick Ludwigshafen Fm. is dominantly fine-grained) thick interval of, sometimes organic-rich or peaty, silts and clays (Gabriel et al., 2013). Following the hypothesis of mostly tectonically controlled deposition, its accommodation results from subsidence resulting in a high (relative) local base level, suggesting continuous deposition. Considering its thickness in light of the large catchment area of the Rhine and Neckar feeding into the Heidelberg Basin, we propose that it should, at least in the vicinity of the investigated site, further represent a relatively short time period on the order of ~10 ka. Both are in concert with the generally homogeneous sedimentary facies, with pollen and gastropod findings, and with only small increases in protein decomposition with depth (see below).

However, previous studies paint a more intricate picture of the pal-ustrine deposits as a much more complex unit. Its fossil content represents, at different locations, either warm-interglacial (e.g. at Ludwigshafen P35 borehole) or cold-glacial (e.g. at Viernheim borehole) environmental conditions (Wedel, 2009). Moreover, it contains at least

two different interglacial mollusc assemblages (Engesser and Münzing, 1991; Rähle, 2005), and at least four different interglacial pollen assemblages (Knipping, 2008). If these interpretations pertain, the palustrine deposits must be considered as a time-transgressive unit covering a considerable time span of one to several hundred ka. It would appear to be a patchwork of non-correlative packages of fines that are the result of episodic, relatively small-scale deposition, and potentially also erosion. This depositional model agrees with luminescence data indicating an age of ~400 ka below, and ~300 ka above the palustrine deposits (and an overlying discontinuity) in Eppelheim (section 5.2.1.; cf. Lauer et al., 2010, 2011; Gabriel et al., 2013; Li et al., 2018), but it is not easily reconciled with the general tectonic and stratigraphic setting. Lang et al. (2011) provide field evidence for local-scale reverse faulting, and thus relative uplift, from the URG margin at Darmstadt (50 km to the north). Although a more frequent and larger-scale occurrence of such tectonic movements seems questionable, they might be a factor for observed heterogeneity in the palustrine deposits and, generally, for observed hiatuses in the URG. It is worth mentioning that in Eppelheim (and likely also in Heidelberg Uni Nord 1; Ellwanger et al., 2009), a hiatus (with palaeosol developed) is discernible only at the top of the palustrine interval, whereas IR-RF dating results from Viernheim indicate an age gap directly underneath it, and only there (Lauer et al., 2011).

## 5.2. Chronology of depositional phases

### 5.2.1. Luminescence dating

It should be noted that luminescence dating of early Middle Pleistocene deposits is not straightforward and that the ages reported here have to be interpreted with caution. Furthermore, as the drilling was not undertaken with the intention of detailed scientific analyses and only the dried-out core could be logged and sampled, we have no reliable information regarding the water content during burial. This was compensated by using large uncertainties in the dose rate calculations. Nevertheless, the available ages provide some interesting insights into the deposition chronology (Table 2, Fig. 2).

The two luminescence ages from the basal part of the Ludwigshafen Fm. (EPP-1, EPP-2) fall into the period of ~550-500 ka, corresponding to MIS 14 to 13 (563–478 ka) which likely represents the final part of the Cromerian (Böse et al., 2012). Assuming the pIRIR ages do not substantially underestimate, this would indicate that in Eppelheim most of the Cromerian is condensed or missing as the underlying Viernheim Fm. is likely older than the Matuyama–Brunhes boundary (Scheidt et al., 2015). The middle part of the Ludwigshafen Fm. is dated to ca. 424 ka (EPP-3, EPP-4), which corresponds to the transition from MIS 12 to 11. This would place the fine-grained palustrine deposits into MIS 11 (424–374 ka), which is consistent with pIRIR results reported by Li et al. (2018) for the Heidelberg Uni Nord sequence. The four luminescence ages from the lower part of the following Mannheim Fm. (EPP5- to EPP-8) have a mean age of 284 ± 10 ka and correlate with MIS 8 (300–243 ka), while in its middle part, one pIRIR age lies out of stratigraphic order (EPP-9). With regard to the fossil content that is indicative of late glacial conditions (section 5.4.), we consider the upper age of 243 ± 21 ka at ~24 m depth (EPP-10) reliable, placing the lower half of the Mannheim Fm. at Eppelheim into MIS 8. In the upper Mannheim Fm., a sample sandwiched between two thick coarse-grained packages (EPP-12) dates to MIS 3 (57–29 ka).

These luminescence results are in excellent agreement with previous radiometric age constraints on the two formations. Lauer et al. (2011) presented IR-RF ages from the nearby Ludwigshafen P34 and Viernheim drillings that attribute the uppermost fluvial deposits of the Ludwigshafen Fm. to ~400 ka, and the base of the Mannheim Fm. to ~300 ka. Their samples correlate roughly to EPP-3/-4 and EPP-5, respectively. In the Heidelberg Uni Nord 1 core, the fluvial Ludwigshafen Fm. was dated to ~450 ka by pIRIR (Li et al., 2018). These agreements are striking and thus, we tend to consider our luminescence dating results reliable despite the above-mentioned challenges. However, we cannot rule out a possible underestimation of pIRIR ages due to fading.

### 5.2.2. Amino acid geochronology

Additional chronological constraints stem from the IcPD data of bithyniid opercula from the palustrine section (between luminescence samples EPP-4 and EPP-5). Although the two analysed taxa, *B. tentaculata* and *P. crassitesta*, are only directly comparable at a small number of horizons (Tesakov et al., 2020), they show statistically similar levels of protein decomposition, and so the assumption is they can be used together to build regional aminostratigraphies.

The extent of protein decomposition in the opercula increases only little with depth, suggesting that the palustrine succession represents a relatively short time span. It has been compared to currently published German and Dutch Middle and Early Pleistocene material. We display here the values of the slow racemiser valene (Val) as they provide the best temporal resolution for the samples in question (Fig. 7). The extent of IcPD in Eppelheim samples is significantly greater than that of samples from Bilzingsleben, Thuringia, and Löwenbrauerei, Berlin, which are attributed to the Holsteinian (Skompski, 1982; Bridgland et al., 2006; Georgopoulou et al., 2015; Lauer et al., 2021) but smaller than that of samples from Bavel in the Netherlands (Penkman et al., 2013), which is the type site for the Bavelian Interglacial (~1.0 Ma; Zagwijn and De Jong, 1984). This confirms that the palustrine deposits in Eppelheim are Middle Pleistocene, and indicates they are older than the Holsteinian but younger than the Bavelian. Interestingly, samples from Voigtstedt, collected from a unit that has been attributed to MIS 29–21, which covers large parts of the Bavelian (Litt et al., 2007), show degrees of racemisation that are significantly different from those at Bavel (Maul et al., 2013). These samples are very similar to our samples (Fig. 7).

The comparator sites are between 300 and 500 km away (Fig. 8), which will result in slight differences in temperature history since burial and, as the rate of protein decomposition increases exponentially with rises in temperature (cf. Hare and Mitterer, 1968; Penkman et al., 2008), in apparent age between the sites (Miller et al., 1999; Wehmiller et al., 2000; Penkman et al., 2011; Tesakov et al., 2020). Due to latitudinal differences in surface climate, the effective diagenetic temperature experienced by the samples differs. To explore the likely magnitude of this, we have compared IcPD data from contemporaneous deposits over a much larger distance and latitudinal gradient, namely the southern UK and the East European Plain (EEP). The difference in IcPD between the UK MIS 11 (Penkman et al., 2011, 2013) and the EEP MQR3 opercula (Tesakov et al., 2020), both dated to ~400 ka, is much smaller (THAA Val D/L mean differences of ~0.06) than between the Bilzingsleben Holsteinian and Eppelheim samples (THAA Val D/L mean differences of ~0.13). This indicates the higher IcPD in the Eppelheim samples is not due to substantial differences in surface temperature.

Another factor regarding diagenetic temperature is geothermal heating. The opercula studied here were found 55–58 m below the surface. Nelson et al. (in prep.) have developed an aminostratigraphy for the Pannonian Basin (Hungary), an area which possesses many similarities to the URG, as it is undergoing subsidence and also has a steep geothermal gradient (45–55 °C/km). Quaternary deposits extend to 600 m, and opercula have been analysed from horizons down to >460 m below surface. Samples down to a depth of ~50–60 m do not show significant geothermal heating impact on the extent of IcPD; this factor does not seem to be significant until depths of ~80 m are reached. This suggests that it is rather unlikely the Eppelheim samples were buried at sufficient depth for the burial temperature to significantly affect IcPD. The amino acid data therefore supports the palustrine deposits in Eppelheim being older than the Holsteinian, rather than there being a substantial temperature difference between the comparator horizons.

### 5.2.3. Biostratigraphic considerations

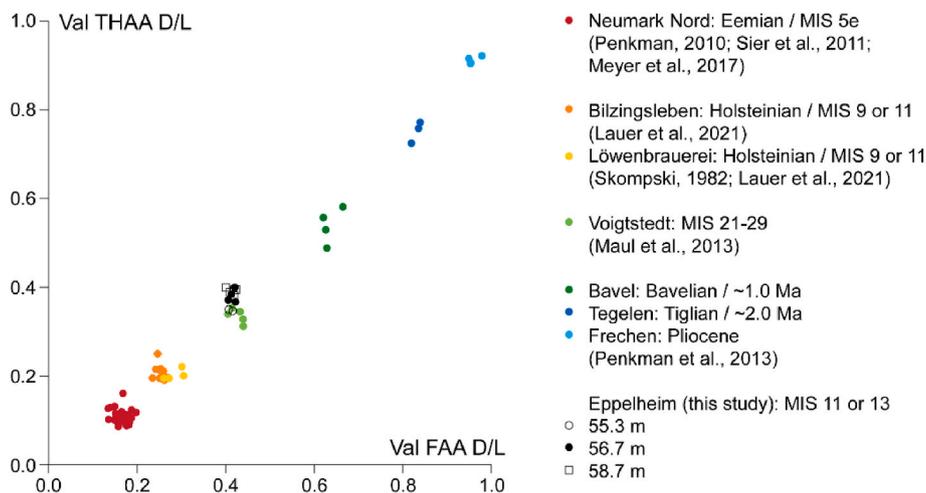#### 5.2.3.1. Molluscs. In Eppelheim, the encountered gastropod

**Fig. 7.** (colour online). Mean D/L FAA vs. THAA for valene of samples from Eppelheim and from other German and Dutch sites. The comparison suggests that the palustrine deposits in Eppelheim are older than the Holsteinian (correlated with MIS 11 by Lauer et al., 2021), but younger than the Bavelian (~1 Ma; see text).



**Fig. 8.** (colour online). Location of Eppelheim (red dot) and reference sites mentioned in the text (yellow: aminostratigraphy, blue: biostratigraphy). NL = Netherlands, CH = Switzerland.

assemblages contain only few biostratigraphically sensitive species. Today, the drill site is located at the western margin of the distribution of the humid forest species *Perforatella bidentata* (Welter-Schultes, 2012). In the southern URG it is absent at present, and Münzing (1976) considered it a pre-Eemian (MIS 5e, 123–109 ka) species, although it has continuously occurred to the southeast, around Stuttgart, after the Eemian (Reiff, 1965; Münzing, 1969). The aquatic taxon *Bithynia transsilvanica* is today encountered only in Eastern Europe, northern Germany and Denmark. In the Netherlands it has been absent throughout the Holocene, occurred only very rarely during the Eemian, but abundantly during the Early Pleistocene (Gittenberger et al., 1998). To our knowledge, it has not previously been reported from the URG. While the data situation precludes definite statements, both species are assumed to be indicators of a pre-Eemian setting. This is supported by the occurrence of *Gyraulus riparius*, known from Early Pleistocene as well as Holocene deposits in the Netherlands (Gittenberger et al., 1998), but only from Middle Pleistocene deposits in the URG (Geissert, 1967). Rähle (2005) reported it from the same lithostratigraphical unit (which he tentatively attributed to the late Cromerian, MIS 15 to 13) from the

Mannheim area (Fig. 8), together with the extinct species *Parafossarulus crassitesta*. The latter occurs sporadically at a distinct level in the Ludwigshafen Fm. referred to as 'crassitesta horizon' (Rähle, 2005; Wedel, 2009), which thus likely corresponds to LMZ 6 at Eppelheim. In the Netherlands, *P. crassitesta* is reported to have become extinct by the Holsteinian (Meijer, 1989).

*5.2.3.2. Pollen.* In contrast to the mollusc zones, the local pollen zones 4–7 (57.8–55.1 m depth) are sufficiently rich in both taxa and specimens to allow more confident correlations with previously published profiles (Fig. 8), although the Eppelheim pollen profile has to be regarded as incomplete, as the early and the late forestation phase are both missing (due to higher-energy deposition and a hiatus, respectively). Still, a correlation with the Early Pleistocene as represented in the clay of Jockgrim (~50 km SW; Kolumbe, 1960; Müller-Stoll, 1985; Peters, 1965) or in two interglacials in a drill core from Schifferstadt (~20 km W, and likely also in Ludwigshafen, ~20 km NW; Knipping, 2008) is highly unlikely due to the lack of 'Tertiary-relict' elements in Eppelheim,

such as *Tsuga, Eucommia, Pterocarya, Carya, Liquidambar*, and *Sciadopytis*. Von der Brelie (1982) studied other Early Pleistocene sections in the wider study area, but unfortunately the results gained are not suited for comparisons because most of the author's drill cores are just represented with one analysed sample. The pollen profile of the late Early Pleistocene Arternian Interglacial from Voigtstedt (Erd, 1970; see also Maul et al., 2013), which is aminostratigraphically very similar to the palustrine section in Eppelheim (see above), unfortunately does not cover the entire forest succession and is therefore not suited for further correlations.

A correlation of the Eppelheim pollen profile to the two oldest interglacials belonging to the Cromerian complex can be excluded due to the lack of *Eucommia* (Osterholz warm stage; Grüger, 1967) and a different forest succession, especially regarding the Hunteburg warm stage (Hahne et al., 1994; Hahne, 1996). Knipping (2008) also investigated deep drill cores from the city of Mannheim (~15 km NW) and described a new thermomere, the so-called Mannheim Interglacial, from sediments that are part of the palustrine deposits. Correlative pollen profiles with the same facies likely occur in two drill cores from the Ludwigshafen area as well, which were however only partly analysed (Knipping, 2008). The Mannheim Interglacial pollen assemblages show an *Alnus* dominance in the lower part and the spread of *Abies* accompanied by high *Alnus* proportions in the upper part. There, *Fagus, Celtis,* and *Azolla* were registered, too. Throughout the entire pollen profile thermophilous deciduous trees occur. This interglacial thus shows clear similarities in the vegetation development compared to that at Eppelheim. The Mannheim Interglacial was tentatively correlated (Knipping, 2008; Weidenfeller and Knipping, 2009) with the Rhume (or Bilshausen) Interglacial (Müller, 1965, 1992) and the Kärlich Interglacial (Urban, 1983; Bittmann, 1991; Bittmann and Müller, 1996). Both are biostratigraphically assigned to the late Cromerian. For the former, a minimum age of ~300 ka exists (IR-RF; Degering and Krbetschek, 2007; Kühl and Gobet, 2010), but the latter has been dated to ~400 ka by $^{40}Ar/^{39}Ar$ (Van Den Bogaard et al., 1989; Bittmann, 1992).

Another potential candidate for a time-equivalent of the Eppelheim pollen record could be the Holsteinian Interglacial. A reference site exists in the Lower Rhine area west of Düsseldorf (Korschenbroich, Hahne et al., 2012), and another in the Eifel region (Döttinger Maar, Diehl and Sirocko, 2007), as well as two Holsteinian pollen diagrams from the northern Alpine foreland (Samerberg, Grüger, 1983; Thalgut, Drescher-Schneider, 2000). During the climatic optimum of this warm stage, forests mainly consisting of *Abies* with an understory rich in *Buxus* were dominant. Subsequently, a distinctive phase with *Fagus* and *Pterocarya* followed. Unfortunately, the Eppelheim pollen record does not cover the entire forest succession of the interglacial (the succession ends with a hiatus), and consequently, it is possible that the immigration of *Pterocarya* is not preserved. However, from a palynostratigraphical point of view, it seems to be more likely that the profile of Eppelheim represents the Mannheim Interglacial and that it is not identical to the Holsteinian (cf. Knipping, 2008). A correlation with the Eemian (Schloss, 2012) can be ruled out because of the occurrence of *Fagus* and *Azolla* as well as the two single findings of *Celtis*.

### 5.2.4. Addressing the conundrum

In summary, the majority of biostratigraphic evidence in the Eppelheim record, as well as at other sites in the vicinity of the Heidelberg Basin (e.g. Rähle, 2005; Knipping, 2008), support a placement of the palustrine succession into the Cromerian (correlated to MIS 21–13, 866–478 ka; Böse et al., 2012). This is supported by amino acid geochronology, where the extent of protein decomposition within the samples is indicative of an age greater than the Holsteinian. In contrast, the luminescence data point toward a younger age, equivalent to MIS 11 (424–374 ka). Previous dating efforts (Lauer et al., 2011; Li et al., 2018) as well as the suggested correlation with the Kärlich interglacial support this younger age range, as the latter has been dated to ~400 ka (Van Den Bogaard et al., 1989; Bittmann, 1992). MIS 11, in contrast, is widely

assumed to correspond to the Holsteinian Interglacial (Lauer and Weiss, 2018; Candy et al., 2024), which according to Hahne et al. (2012) is remarkably absent in most pollen profiles from the URG, and does not fit with the Mannheim and Kärlich interglacial pollen.

Following this evidence, we offer three possible explanations. First, the luminescence chronology is correct, but the vegetation at the time was not typical of the Holsteinian. As the Upper Rhine area is characterised by a regional climate that is warmer and milder than in surrounding areas at present (Deutscher Wetterdienst, 2022), this probably also applied to substantial periods of times in the past. As a result, this might have favoured a different regional vegetation development. The Upper Rhine area may have been a refugium where Cromerian taxa could outlast the pronounced cold period of MIS 12 (474–424 ka) and expand again afterwards, developing a late Cromerian-type vegetation during MIS 11 (cf. Birks and Willis, 2008). If this holds true, the species composition encompassed several thermophilous trees such as *Corylus, Quercus*, and *Ulmus*, which survived the preceding cold stage. Possibly this was favoured by the occurrence of hot springs in the Upper Rhine Graben area providing a humid and warm microclimate in the close surroundings (Hošek et al., 2024). Second, the luminescence chronology is correct, but the correlation of the Holsteinian Interglacial (or all Holsteinian-type pollen sequences; Scourse, 2006) to MIS 11 may not be supported, as has been suggested by Geyh and Müller (2005) based on U/Th ages corresponding to MIS 9 (337–300 ka) from the type area of the Holsteinian Interglacial. In the Eppelheim core, we observe a major hiatus – palaeosol, sharp facies change, and a 150 ka-gap in the luminescence ages – covering this time interval. This hiatus appears to occur widespread in the Heidelberg Basin, which would explain the regional lack of clear Holsteinian pollen profiles noticed by Hahne et al. (2012), assuming its correlation to MIS 9 to be correct. Third, luminescence ages could systematically underestimate the real age of deposition, and the palustrine deposits could in fact be of Cromerian age. This might be related to fading of the luminescence signal or other effects and it will require further studies to investigate this.

### 5.3. Environmental reconstruction

The palustrine deposits in Eppelheim contain a rich archive of environmental indicators, including diverse mollusc assemblages. Together with palynological findings, the ecological tolerances of encountered mollusc species according to national and international reference atlases allow a rough characterisation of climatic boundary conditions and the common habitat. For this, we refer to Falkner et al. (2002), Germain (1930, 1931), Gittenberger et al. (1998), Horsák et al. (2013), Kerney et al. (1983), and Welter-Schultes (2012).

Despite a remarkable richness of 21 taxa (Fig. 5), especially regarding the small sample volumes available from the drill cores, LMZ 1 (62.9–61.3 m) reflects transitional conditions, as molluscan faunas from full interglacial forest optimums are even more diverse (Limondin-Lozouet and Preece, 2014) and typical interglacial taxa are absent here. Terrestrial species indicative of an open riverine forest and humid-temperate conditions occur (*Cepaea* sp., *Oxychilus* cf. *Cellarius, Carychium minimum, Cochlicopa* cf. *nitens, Perforatella bidentata, Clausilia* cf. *pumila*). The corresponding lower part of LPZ 1, with 40–50 % of arboreal pollen, mainly *Pinus* and *Betula*, supports an open and sparsely vegetated environment (Fig. 4). Aquatic gastropods are mostly indicative of vegetated, standing waters and/or periodic swamps, while species indicative of moving waters (*Bithynia tentaculata, Valvata piscinalis*) occur only below 62.0 m. In LMZ 2 (61.3–60.9 m), which represents the top of the first fining-upward cycle (Fig. 3), the terrestrial component is characterised by species typical of a humid tundra environment as well as the glacial taxa *Pupilla alpicola* and *Vallonia tenuilabris*. Though this last species presently occur in Siberian taiga (Schileyko, 1984; White et al., 2008) and in the Baikal area in Holocene floodplain deposits of both Lena (White et al., 2008) and Selenga (White et al., 2013) rivers, the Eppelheim assemblage is much less diversified than these latter and

similar to that of Late Pleistocene loess molluscan faunas in western Europe as reported by Moine (2014) and may be representative either of early glacial or early lateglacial conditions, or a cold stadial (Fig. 9), which is in line with a decline of arboreal pollen to ~30 % (upper LPZ 1). The full-glacial taxa disappear in LMZ 3 (60.8–59.6 m), while *Perforatella bidentata*, typical of humid forests (e.g. Wedel, 2009), and the mesophilous species *Oxychilus* cf. *Cellarius* reappear. At the same time, arboreal pollen become again more abundant, altogether indicating a re-established forest tundra. The few aquatic gastropods attest to the presence of temporary water bodies only.

The assemblage of LMZ 4 (59.5–58.4 m; Fig. 5) reflects a river margin with aquatic vegetation (e.g. *Myriophyllum*, Fig. 4). The occurrence of mussels (*Unio* sp.) and rounded fragments thereof in the lowest part (below 59.3 m) points toward a flowing stream. Above, species of standing and/or temporary water bodies (e.g. *Anisus spirorbis, Stagnicola palustris, Planorbis, Gyraulus crista*) become dominant. However, the abundant opercula of *Bithynia tentaculata* that are much more frequent than the corresponding shells suggest their enrichment by currents at 58.8–58.4 m (Bennike et al., 1998; Gilbertson and Hawkins, 1978). They occur together with relatively small amounts of Characeae oogonia. Such co-occurrence has also been observed in the submerged vegetation zone of the Furesø lake in Denmark (Wesenberg-Lund et al., 1917). Supernumerary opercula and Characeae oogonia are thus assumed to be of allochthonous origin, as such discrepancy does not affect material of *Bithynia transsilvanica* known to live in semi-permanent shallow waters. It is difficult to propose a climatic context for this zone, as climatic tolerances of present mollusc taxa are either wide or still partly unknown (e.g. *Bithynia transsilvanica*). LMZ 4 terminates with a second impoverishment of the floral assemblages indicating another transition from forested to open conditions (LPZ 3), and the onset of a new fining-upward cycle.

*Cepaea* sp. and *Oxychilus* cf. *Cellarius* in LMZ 5 (58.2–56.6 m) indicate temperate but not fully interglacial conditions (supported by cf. *Aegopinella nitidula* and *Helicigona lapicida*) and at least the presence of shrubs at the site, likely with woods in the surroundings. In fact, the corresponding LPZ 4–6 represent a thermophilous forest with, among others, *Alnus, Ulmus*, and *Corylus*, that points toward nearly full interglacial conditions. The continuous presence of *Anisus spirorbis* attests to temporary water bodies. The environment changes slightly above ~57 m, indicated by an increase in species richness with more open humid forest taxa (e.g. *Vitrea crystallina, Arianta arbustorum,* and *Perforatella bidentata*), and where *Bithynia tentaculata* and *Valvata piscinalis* indicate permanent, potentially flowing water. LMZ 5 occurs in a sediment that is remarkably enriched in $CaCO_3$ (from ~20 to ~50 %) compared to the remainder of the fine-grained sequence (Fig. 3). As TOC is, at the same time, visibly reduced, this suggests a phase with an increased sedimentation rate.

Between 56.6 and 55.6 m, no shell fragments are encountered, but the pollen composition is indicative of a dense interglacial forest with high abundances of *Abies* and *Alnus* (LPZ 7). At the same time, frequent roots as well as a steep increase in TOC occur. It is unlikely that no gastropods were present under conditions that favoured a diverse vegetation growth, therefore we suggest that shells were initially present but dissolved by humic acids. This is supported by very low $CaCO_3$ concentrations in the sediment matrix (mostly <5 %). Mainly aquatic taxa adapted to both temporary (*Anisus* spp.) and permanent, stagnant (*Gyraulus crista, Valvata* spp.) or running (*Bithynia tentaculata, Parafossarulus crassitesta*), water bodies appear in LMZ 6 (55.6–55.1 m). This suggests a depositional environment near the margin of a stream, with a rich aquatic vegetation (Fig. 9). The frequent findings of *Azolla* are indicative of warm and sub-oceanic conditions. Throughout this interval, the sediment grain size increases slightly, which could point toward a moderately increasing current.

Overall, an alternation of dominantly terrestrial (LMZ 1–3, 5) and aquatic (LMZ 4, 6) mollusc assemblages can be observed within the palustrine deposits (Fig. 5). Therefore, the respective interval at EPP cannot be regarded as an exclusively lacustrine sequence, which differs from earlier suggestions for boreholes further north in the Heidelberg Basin (Gabriel et al., 2013, and references therein). Rather, it appears that the majority of the fines were deposited in a palustrine setting, likely in a floodbasin fed by overbank flow spills. Repeated changes in base level might well be indicators of distinct tectonic movements. At 55.0 m, the fines are abruptly truncated, and overlain by predominantly sandy deposits (Fig. 3). These contain LMZ 7 (55.0–54.0 m) that is characterised by poorly preserved specimens with worn shell surfaces, holes, and brownish incrustations, all of which points toward reworking by a higher-energy current, and potentially a significant hiatus in between.

Further up the sequence, LMZ 8 (25.5–24.2 m) comprises mainly terrestrial taxa with frequent occurrences of *Trochulus hispidus* and
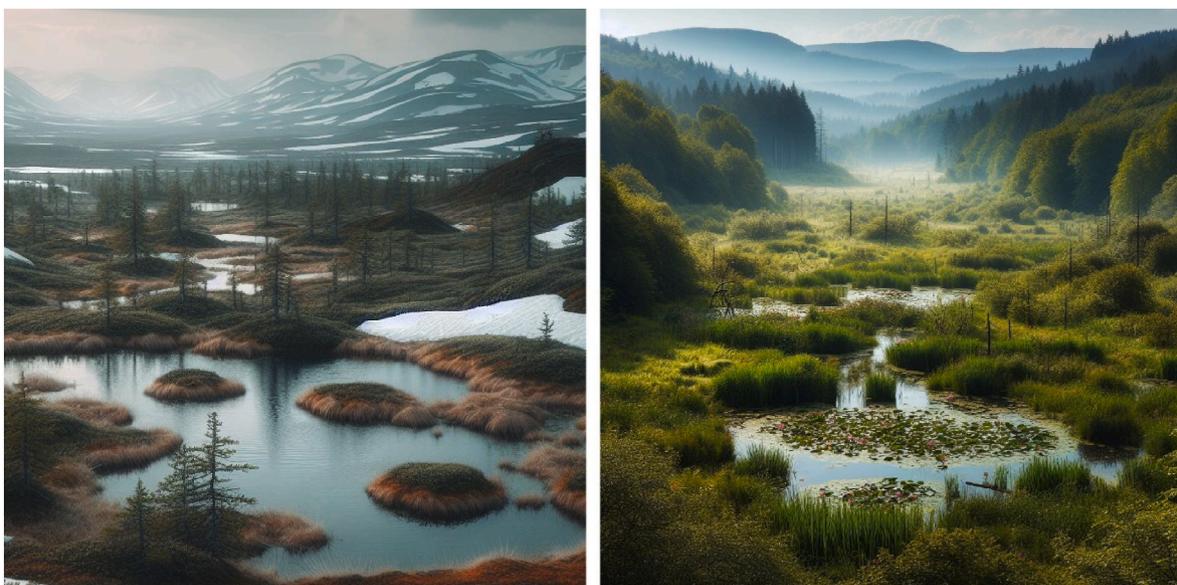


**Fig. 9.** (colour online). Environmental indicators in the interval at 64-55 m depth, mainly mollusc shells and pollen, suggest a transition from a sparsely vegetated, cold setting with open forest tundra (left) toward full interglacial conditions with a thriving forest and diverse aquatic vegetation (right) during the sediments' deposition. Illustrations made with DALL·E 3 (via www.bing.com/images/create, last accessed 02.05.2024).

*Vallonia costata*, which are both indicators of rather cool but not glacial climatic conditions, and an open meadow landscape. Replacement of *Vallonia pulchella, Cochlicopa lubrica,* and *Succinella oblonga* by *Pupilla muscorum* points toward a slight decrease in humidity. This assemblage is similar to some Late Glacial successions presented by Limondin-Lozouet (1998, 2002).

### 5.4. Tectonic versus climatic controls on sedimentation

Two compositional endmembers are encountered both in the gravel and sand fractions of the EPP drilling. One is characterised by clasts of red sandstones and grey limestones (Fig. 2) derived mainly from the Lower Triassic ('Buntsandstein') and the Middle Triassic ('Muschelkalk'), respectively, which occur in large parts of the Neckar drainage area (Fig. 1; Ellwanger et al., 2009; Simon, 2012). Some light limestones may also originate from the Jurassic of the Swabian Alb further upstream. In parts, these lithologies have probably been delivered into the Heidelberg Basin by short-travelled mass flow events, especially where they occur in poorly sorted and poorly rounded diamicts ('local provenance' in Ellwanger et al., 2009; not explicitly distinguished here). The corresponding Neckar-facies sand is reddish, rather coarse-grained and angular, due to comparatively low fluvial transport distances (Fig. 9). In other sections, the gravel is dominated by blackish, frequently siliceous limestones, variants of $SiO_2$ (quartzite, vein quartz, chert) and crystalline rocks, which are typical of Alpine rocks, and thus of the headwaters of the Rhine river (Fig. 1; Hoselmann, 2009; Gegg et al., in review). This Rhenish material is mostly rounded and further includes inputs from the Molasse Basin (mainly calcareous sandstones and $SiO_2$ variants), the lower mountain ranges of the Vosges and the Black Forest, and their foothills (mainly crystalline rocks but also some Triassic and other

sedimentary rocks; Berger et al., 2005; Skrzypek et al., 2014; Gegg et al., in review). Rhenish sand is greyish, with finer and better-rounded grains, and is thus attributed to the Rhine river (Ellwanger et al., 2009; Hoselmann, 2009). It is noteworthy that the Neckar-type sand shows very low to no carbonate content despite a large portion of the Neckar drainage area consisting of Triassic and Jurassic limestone, while the Alpine-derived Rhine-type sand contains a notable carbonate content as well as characteristic flakes of muscovite (Ellwanger et al., 2009; Hoselmann, 2009; Gabriel et al., 2013).

This fluvial facies subdivision is supported by correlation analysis of the encountered lithology groups (Fig. 10A). While the lithologies attributed to the Rhine facies show strong positive correlations among each other, they are inversely correlated with rocks attributed to the Neckar facies. Among Neckar-facies lithologies, correlation coefficients are lower. This might be due to some of the Triassic sediments being delivered by the Rhine river from small, more southerly tributaries (e.g. rivers Kinzig and Murg), but also due to heterogeneity among the Neckar-derived samples, i.e. the existence of discrete sub-facies. The latter is also suggested by principal component analysis (Fig. 10B). Non-calcareous sandstones show no correlations to most other lithology groups and might also have been delivered by both rivers.

It has been suggested that the E-W drainage pattern within the URG is, to a large extent, tectonically controlled, and that a general eastward shift of the Rhine over the entire Pleistocene is caused by subsidence of the Heidelberg Basin, which is strongest at the eastern graben margin (Figs. 1 and 8; Hagedorn and Boenigk, 2008; Weidenfeller and Kärcher, 2008, Weidenfeller and Knipping, 2009). In contrast, during episodes of quiescence, as appears to be currently the case (Fuhrmann et al., 2013, 2015), sediments delivered from the Neckar river would develop a westward-prograding alluvial fan that would rather deflect the Rhine in
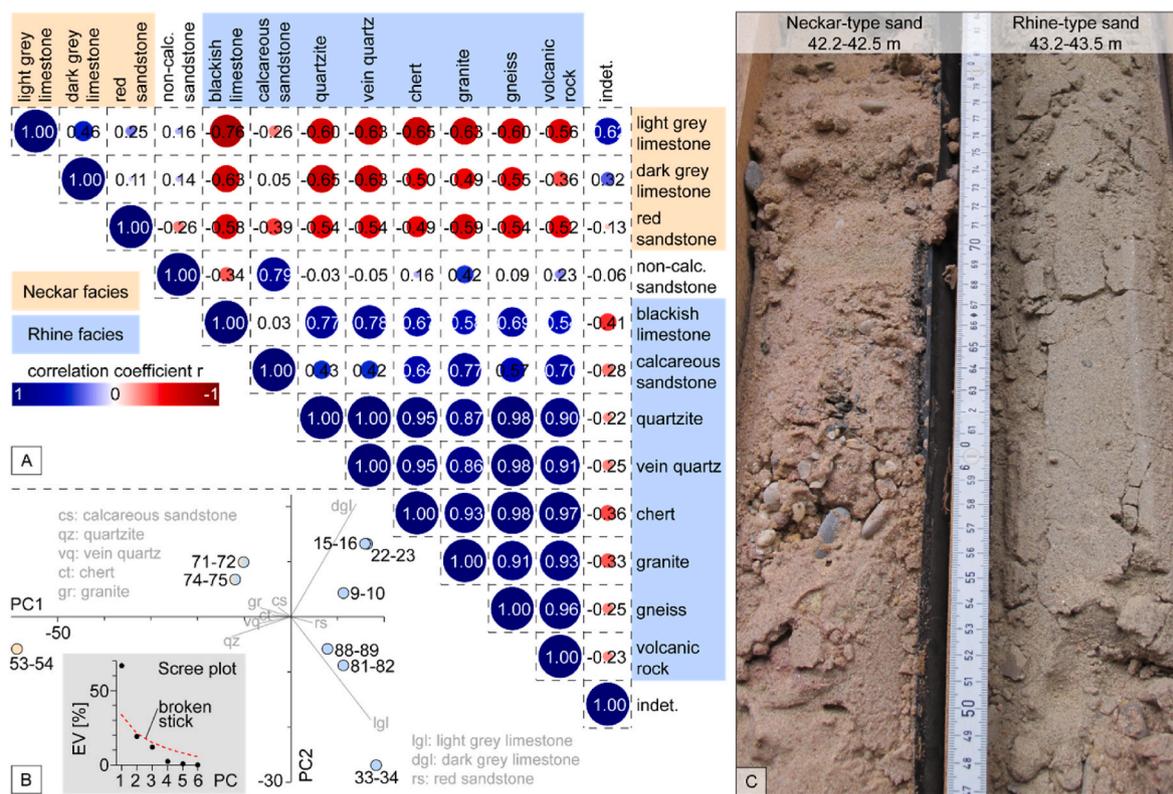


**Fig. 10.** (colour online). Characterisation of Neckar and Rhine sedimentary facies. A) Correlation plot of clast lithologies in gravel samples supporting the distinction of Neckar (blue) and Rhine contributions (orange; see also Fig. 2). 1 = perfect correlation, 0 = no correlation, −1 = perfect anti-correlation. B) Principal component analysis of gravel samples based on petrographic composition, labels correspond to sampling depth in metres. PC1 separates Rhine-from Neckar-dominated samples (low and high PC1 score, respectively), PC2, although below significance threshold, indicates the presence of at least two Neckar sub-facies. C) Comparison of Neckar- (left; reddish, medium-coarse, frequently angular, carbonate-free) and Rhine-type (right; greyish, fine-medium, mostly rounded, carbonaceous) sand fractions.

the opposite direction (Fig. 11; Ellwanger et al., 2009; Löscher et al., 1980; Przyrowski and Schäfer, 2015). Following this line of reasoning, the predominantly Neckar-dominated facies in the Viernheim Fm (Fig. 2). would indicate relative tectonic quiescence during the Early Pleistocene. In the overlying Ludwigshafen Fm., the Rhine influence increases steadily, pointing towards accelerated Heidelberg Basin subsidence during the Middle Pleistocene. A layer of pure Rhenish sand is overlain by a thick unit of fines at 64-55 m that according to Gabriel et al. (2013) are of Rhenish origin as well. Their widespread occurrence in the Heidelberg Basin, which may at times have extended some 15 km up into the Neckar valley (Ellwanger et al., 2009), is further evidence of regionally vastly increased accommodation space resulting in the formation of extensive floodbasins and possibly, closer to the centre of subsidence, lakes. The average sedimentation rate throughout the Ludwigshafen Fm. is ~0.2 mm/yr.

The lower half of the Mannheim Fm. indicates another phase of subsidence, possibly during MIS 8, with a sedimentation rate of ~0.5 mm/yr (Fig. 2). The switch to an exclusive Neckar provenance at ~40 m depth documents a new phase of alluvial fan progradation into the Heidelberg Basin, which reached far into the basin centre (Viernheim drilling ~20 km to the north; Hoselmann, 2009; Gabriel et al., 2013). It indicates a subsidence slowdown in late MIS 8 that is accompanied by a drop in sedimentation rate to ~0.1 mm/yr. This quiescence following an episode of drastic subsidence is further supported by a near-identical depth to the top of the Ludwigshafen Fm (56 m vs. 55.0 m in EPP). in the neighbouring borehole Heidelberg Uni Nord (Fig. 1; Ellwanger et al., 2009), while there, closer to the centre of subsidence, its base lies significantly deeper (126 m vs. 87.4 m in EPP). Similar observations have been made by Weidenfeller and Knipping (2009) comparing the drillings Ludwigshafen-Parkinsel P34 and P35. Interestingly, our luminescence data suggest that in between two periods of subsidence in the Ludwigshafen Fm. and Mannheim Fm., a hiatus exists that spans MIS 10 to 9. Similar findings have been made in previous studies and are not trivial to explain (sections 5.1.2., 5.2.4.).

A second major controlling factor for deposition in the URG is the highly variable climate throughout the Quaternary. This applies especially (but not exclusively) to the Rhine system, whose headwaters were frequently and extensively glaciated (Preusser, 2008; Ellwanger et al., 2011; Schlüchter et al., 2021), resulting in periodic pulses of meltwater traversing the URG and delivering glacially and periglacially eroded debris (e.g. Leeder et al., 1998; Cordier et al., 2017; Erkens et al., 2009). Some 20 km to the south at Kronau, Preusser et al. (2021) encountered repeated packages of Rhine-derived gravels that can be correlated with Alpine glaciations. This implies that at this position, the deposition in the URG is, at least to a significant degree, climatically controlled. Although the record at Eppelheim covers more or less the same time span, we do not observe a similarly clear depositional pattern of glacial-interglacial dynamics. However, significant occurrence of Alpine material in the Ludwigshafen Fm. starts, according to luminescence

data, at ~500 ka and continues through MIS 12 (Fig. 2). MIS 12 was a pronounced global cold phase (Lisiecki and Raymo, 2005) associated with major northern hemisphere glaciations (e.g. Gibbard and Clark, 2011; Böse et al., 2012), and most likely the timing of the Most Extensive Glaciation in the (western/central) Alps (Preusser et al., 2011, 2021; Schlüchter et al., 2021; Dieleman et al., 2022). In the basal Mannheim Fm., Alpine sediment was initially deposited, while later on, only Neckar-derived material occurs. Although the Neckar catchment was presumably never glaciated (e.g. Fiebig et al., 2011), episodes of faster and coarser-grained deposition during cold periods should be expected due to efficient physical weathering and erosion under periglacial conditions (e.g. Braun, 1989; Merritts and Rahnis, 2022). The Eppelheim sequence contains four intervals of especially coarse Neckar deposits between 40 and 5 m depth. While more age constraints in this section would be necessary for definite correlations, we consider it not unlikely that these coarse layers represent the cold periods of MIS 8, 6, 4, and 2 (Fig. 2).

## 6. Conclusions

This study introduces a new, 136-m-long stratigraphic record from Eppelheim in the Heidelberg Basin, northern URG, an area of long-lasting subsidence whose archives can assume a key role for regional, and potentially over-regional, Quaternary stratigraphy. This record comprises fluvial, colluvial, and palustrine sediments that represent at least the last ~500 ka. Good evidence exists of both tectonically and climatically controlled deposition in the Heidelberg Basin, and we argue that the stratigraphic sequence, as well as that at neighbouring sites, needs to be regarded as a product of the interplay of both factors. Phases of quiescence or subsidence influence the spatial pattern of sedimentation, favouring either alluvial fan progradation from the Neckar river (east to west), or migration of the Rhine towards the basin centre (west to east), respectively. This pattern is overprinted by periodically increased coarse sediment yields, especially from the Rhine whose source area was extensively glaciated, during cold phases.

Specific attention is paid to a prominent unit of fines, here ~10 m thick, that occurs widespread in the Heidelberg Basin, but with conflicting interpretations regarding its timing and mode of deposition. On a larger scale, this could be explained by a longer phase of pronounced non-uniform basin subsidence, where individual blocks subside at different times and at different rates, leading to a mosaic of non-correlative but generally similar-facies sediment bodies. In Eppelheim, the fines' diverse gastropod content reveals a mostly palustrine origin compatible with a floodplain setting. Together with pollen assemblages, it illustrates a general trend of initially cold and fluctuating, but continuously ameliorating and finally fully interglacial environmental conditions during their deposition. Palynologically, it is very similar to the (presumed late Cromerian) Mannheim Interglacial as defined close by, whereas a correlation with the (presumed MIS 11) Holsteinian
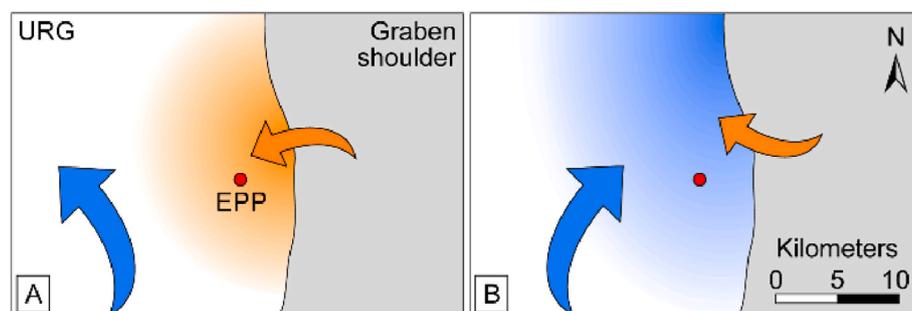


**Fig. 11.** (colour online). Simplified sketch of the tectonic control on deposition in the Heidelberg Basin, northern URG. A) In phases of quiescence (prolonged low subsidence rates), sediment input from the Neckar accumulates a prograding fan (orange arrow) that forms an obstacle for the Rhine and diverts it towards the west (blue arrow). B) In phases of stronger subsidence, the Rhine deflects towards the east. Then, its sediments, either in fluvial or, at very high subsidence rates, palustrine facies, reach the location of the EPP drilling (blue colour, cf. Fig. 1).

Interglacial appears unlikely. While a late Cromerian placement is supported by the amino acid geochronology, our pIRIR ages are younger and correspond to MIS 11, in agreement with previous luminescence studies on correlative deposits in other drill cores. This suggests that the Holsteinian is either i) characterised by an atypical vegetation composition in the Upper Rhine area, ii) that it is in fact younger than often assumed (i.e. MIS 9 rather than MIS 11), or iii) that the luminescence approach underestimates the sediments' depositional age.

Unfortunately, the palustrine succession in Eppelheim terminates with a sharp and potentially erosive boundary, so that the interglacial succession is only partly preserved. This boundary change follows a palaeosol and coincides with a 150 ka-luminescence age gap, suggesting a major hiatus. A more complete succession of the palustrine deposits might be preserved at sites yet closer to the subsidence centre at the eastern graben margin. The search for and investigation of such a site could thus be very beneficial for over-regional Middle Pleistocene stratigraphy. In addition, the hiatus raises the question whether the often-presumed continuity and completeness of the URG infill has been generally overestimated. An allostratigraphic approach, identifying and mapping discontinuities, could be enlightening. In general, future work in the URG needs to take into account varying rates and timings of subsidence (and potentially uplift) in the different sectors of the graben that are challenging to link, as well as the drastic climatic changes that affected the sedimentary systems. The prerequisite for this are additional profiles in high resolution and a combination of different stratigraphic approaches, including robust chronologies.

## CRediT authorship contribution statement

**Lukas Gegg:** Project coordination, Lithostratigraphic analysis, General interpretation, Manuscript draft. **Laura Jacob:** Initial core description, Sampling, Lithostratigraphic analysis. **Olivier Moine:** Evaluation and interpretation of gastropod assemblages. **Ellie Nelson:** Amino acid analysis and interpretation. **Fiona Schwahn:** Initial core description, Sampling, Lithostratigraphic analysis. **Philipp Stojakowits:** Evaluation and interpretation of pollen assemblages. **Dustin White:** Amino acid analysis and interpretation. Ulrike Wielandt-Schuster: Project coordination. **Ulrike Wielandt-Schuster:** Project coordination. Frank Preusser: Project coordination, Luminescence analysis, General interpretation. **Frank Preusser:** Project coordination, Luminescence analysis, General interpretation. All authors: contributions to, approval of the manuscript.

## Declaration of competing interest

Frank Preusser is member of the Editorial Advisory Board for Quaternary Science Reviews and was not involved in the editorial review or the decision to publish this article. Other than that, the authors declare that they have no known competing financial interests or personal relationships that could have appeared to influence the work reported in this paper.

## Acknowledgements

## Data availability

Data will be made available on request.

## References

Abdulkarim, M., Grema, H.M., Adamu, I.H., Mueller, D., Schulz, M., Ulbrich, M., Miocic, J.M., Preusser, F., 2021. Effect of using different chemical dispersing agents in grain size analyses of fluvial sediments via laser diffraction spectrometry. MPs 4, 44. https://doi.org/10.3390/mps4030044.

Bachmann, G.H., Wang, Y., 2014. Armoured mud balls as a result of ephemeral fluvial flood in a humid climate: modern example from Guizhou Province, South China. J. Palaeogeogr. 3, 410–418. https://doi.org/10.3724/SP.J.1261.2014.00064.

Bank, R.A., Bieler, R., Bouchet, P., Decock, W., Dekeyser, S., Kroh, A., Marshall, B., Neubauer, T.A., Neubert, E., Rosenberg, G., Sartori, A.F., Schneider, S., Trias-Verbeek, A., Vandepitte, L., Vanhoorne, R., Gofas, S., 2014. MolluscaBase – announcing a world register of all molluscs. Presented at the 7th Congress of the European Malacological Societies.

Bartz, J., 1974. Die Mächtigkeit des Quartärs im Oberrheingraben. In: Approaches to Taphrogenesis, Inter-Union-Commission on Geodynamics Scientific Report. Schweizerbart, pp. 78–87.

Beccaletto, L., Capar, L., Cruz-Mermy, D., Rupf, I., Nitsch, E., Oliviero, G., Elsass, P., Perrin, A., Marc, S., 2010. The GeORG project - geological potential of the upper rhine graben - situation, goals and first scientific results. In: 23ème RST. Bordeaux, France.

Bennike, O., Lemke, W., Jensen, J.B., 1998. Fauna and flora in submarine early Holocene lake-marl deposits from the southwestern Baltic Sea. Holocene 8, 353–358. https://doi.org/10.1191/095968398673688465.

Berger, J.-P., Reichenbacher, B., Becker, D., Grimm, M., Grimm, K., Picot, L., Storni, A., Pirkenseer, C., Derer, C., Schaefer, A., 2005. Paleogeography of the upper rhine graben (URG) and the Swiss Molasse Basin (SMB) from eocene to Pliocene. Int. J. Earth Sci. 94, 697–710. https://doi.org/10.1007/s00531-005-0475-2.

Beug, H.J., 2004. Leitfaden der Pollenbestimmung für Mitteleuropa und angrenzende Gebiete. Verlag Dr. Friedrich Pfeil, Munich.

BGR, 2006. Geologische Karte der Bundesrepublik Deutschland 1:1.000.000 (GK1000).

Birks, H.J.B., Willis, K.J., 2008. Alpines, trees, and refugia in Europe. Plant Ecol. Divers. 1, 147–160. https://doi.org/10.1080/17550870802349146.

Bittmann, F., 1991. Vegetationsgeschichtliche Untersuchungen an mittel- und jungpleistozänen Ablagerungen des Neuwieder Beckens (Mittelrhein). Jahrb. Des. Romisch-Germanischen Zentralmus. Mainz 38, 83–190. https://doi.org/10.11588/jrgzm.1991.1.84016.

Bittmann, F., 1992. The Kärlich interglacial, Middle Rhine region, Germany: vegetation history and stratigraphic position. Veget Hist Archaebot 1, 243–258. https://doi.org/10.1007/BF00189501.

Bittmann, F., Müller, H., 1996. The Kärlich Interglacial site and its correlation with the Bilshausen sequence. In: The Early Middle Pleistocene in Europe. CRC Press, pp. 187–193.

Bittmann, F., Börner, A., Doppler, G., Ellwanger, D., Hoselmann, C., Katzschmann, L., Sprafke, T., Strahl, J., Wansa, S., Wielandt-Schuster, U., 2018. The quaternary in the stratigraphic table of Germany 2016. Z. Dtsch. Ges. Geowiss. 295–306. https://doi.org/10.1127/zdgg/2018/0123.

Boenigk, W., 1982. Der Einfluss des Rheingraben-Systems auf die Flussgeschichte des Rheins. Zeitschrift für Geomorphologie, Supplementband 42, 167–175.

Bos, J.A.A., Dambeck, R., Kalis, A.J., Schweizer, A., Thiemeyer, H., 2008. Palaeoenvironmental changes and vegetation history of the northern Upper Rhine Graben (southwestern Germany) since the Lateglacial. Neth. J. Geosci. 87, 67–90. https://doi.org/10.1017/S0016774600024057.

Böse, M., Lüthgens, C., Lee, J.R., Rose, J., 2012. Quaternary glaciations of northern Europe. Quaternary Science Reviews, Quaternary Glaciation History of Northern Europe 44, 1–25. https://doi.org/10.1016/j.quascirev.2012.04.017.

Braun, D.D., 1989. Glacial and periglacial erosion of the Appalachians. Geomorphology 2, 233–256. https://doi.org/10.1016/0169-555X(89)90014-7.

Bridgland, D.R., Antoine, P., Limondin-Lozouet, N., Santisteban, J.I., Westaway, R., White, M.J., 2006. The Palaeolithic occupation of Europe as revealed by evidence from the rivers: data from IGCP 449. J. Quat. Sci. 21, 437–455. https://doi.org/10.1002/jqs.1042.

Campbell, J.F.E., Fletcher, W.J., Hughes, P.D., Shuttleworth, E.L., 2016. A comparison of pollen extraction methods confirms dense-media separation as a reliable method of pollen preparation. J. Quat. Sci. 31, 631–640. https://doi.org/10.1002/jqs.2886.

Candy, I., Oliveira, D., Parkes, D., Sherriff, J., Thornalley, D., 2024. Marine Isotope Stage 11c in Europe: recent advances in marine–terrestrial correlations and their implications for interglacial stratigraphy – a review. Boreas n/a. https://doi.org/10.1111/bor.12656.

Chen, Y.W., Li, S.H., Li, B., 2013. Residual doses and sensitivity change of post IR IRSL signals from potassium feldspar under different bleaching conditions. Geochronometria 40, 229–238. https://doi.org/10.2478/s13386-013-0128-3.

Cordier, S., Adamson, K., Delmas, M., Calvet, M., Harmand, D., 2017. Of ice and water: Quaternary fluvial response to glacial forcing. Quaternary Science Reviews, Quaternary fluvial archives: advances from the first 20 years of FLAG (the Fluvial Archives Group) 166, 57–73. https://doi.org/10.1016/j.quascirev.2017.02.006.

Degering, D., Degering, A., 2020. Change is the only constant - time-dependent dose rates in luminescence dating. Quat. Geochronol. 58, 101074. https://doi.org/10.1016/j.quageo.2020.101074.

Degering, D., Krbetschek, M.R., 2007. Dating of interglacial sediments by luminescence methods. Developments in Quaternary Sciences 7, 157–171. https://doi.org/10.1016/S1571-0866(07)80036-4.

Deutscher Wetterdienst, 2022. Nationaler Klimareport, sixth ed.

Dèzes, P., Schmid, S.M., Ziegler, P.A., 2004. Evolution of the European Cenozoic Rift System: interaction of the alpine and pyrenean orogens with their foreland lithosphere. Tectonophysics 389, 1–33. https://doi.org/10.1016/j.tecto.2004.06.011.

Diehl, M., Sirocko, F., 2007. 27. A new holsteinian pollen record from the dry maar at Döttingen (Eifel). In: Sirocko, F., Claussen, M., Sánchez Goñi, M.F., Litt, T. (Eds.), Developments in Quaternary Sciences, the Climate of Past Interglacials. Elsevier, pp. 397–416. https://doi.org/10.1016/S1571-0866(07)80052-2.

Dieleman, C., Christl, M., Vockenhuber, C., Gautschi, P., Graf, H.R., Akçar, N., 2022. Age of the most extensive glaciation in the Alps. Geosciences 12, 39. https://doi.org/10.3390/geosciences12010039.

Drescher-Schneider, R., 2000. 2. Halt: kiesgrube Thalgut: pollen-und großrestanalytische untersuchungen. In: Kelly, M., Linden, U., Schlüchter, C. (Eds.), Exkursionsführer DEUQUA 2000, pp. 128–136.

Ellwanger, D., Gabriel, G., Hoselmann, C., Lämmermann-Barthel, J., Weidenfeller, M., 2005. The Heidelberg drilling project (upper rhine graben, Germany). Quaternaire. Revue de l'Association française pour l'étude du Quaternaire 191–199. https://doi.org/10.4000/quaternaire.406.

Ellwanger, D., Gabriel, G., Simon, T., Wielandt-Schuster, U., Greiling, R.O., Hagedorn, E.-M., Hahne, J., Heinz, J., 2009. Long sequence of quaternary rocks in the Heidelberg Basin depocentre. E&G Quaternary Sci. J. 57 (3), 316–337. https://doi.org/10.3285/eg.57.3-4.

Ellwanger, D., Wielandt-Schuster, U., Franz, M., Simon, T., 2011. The quaternary of the southwest German alpine foreland (Bodensee-Oberschwaben, baden-württemberg, southwest Germany). E&G Quaternary Science Journal 60, 306–328. https://doi.org/10.3285/eg.60.2-3.07.

Engesser, W., Münzing, K., 1991. Molluskenfaunen aus Bohrungen im Raum Philippsburg-Manheim und ihre Bedeutung für die Quartärstratigraphie des Oberrheingraben. Jahreshefte des Geologischen Landesamts Baden-Württemberg 33, 97–117.

Erd, K., 1970. Pollen-analytical classification of the middle pleistocene in the German Democratic Republic. Palaeogeogr. Palaeoclimatol. Palaeoecol. 8, 129–145. https://doi.org/10.1016/0031-0182(70)90006-4.

Erkens, G., Dambeck, R., Volleberg, K.P., Bouman, M.T., Bos, J.A., Cohen, K.M., Wallinga, J., Hoek, W.Z., 2009. Fluvial terrace formation in the northern Upper Rhine Graben during the last 20 000 years as a result of allogenic controls and autogenic evolution. Geomorphology 103, 476–495. https://doi.org/10.1016/j.geomorph.2008.07.021.

Faegri, K., Iversen, J., 1989. Textbook of Pollen Analysis, fourth ed. John Wiley & Sons Ltd.

Falkner, G., Ripken, T.E.J., Falkner, M., 2002. Mollusques continentaux de France. Liste de Référence annotée et Bibliographie, Patrimoines naturels. Muséum national d'Histoire naturelle, Paris.

Fiebig, M., Ellwanger, D., Doppler, G., 2011. Pleistocene glaciations of southern Germany. In: Developments in Quaternary Sciences. Elsevier, pp. 163–173.

Frey, M., Bär, N., Stober, I., Reinecker, J., van der Vaart, J., Sass, I., 2022. Assessment of deep geothermal research and development in the Upper Rhine Graben. Geoth. Energy 10, 18. https://doi.org/10.1186/s40517-022-00226-2.

Fuhrmann, T., Heck, B., Knöpfler, A., Masson, F., Mayer, M., Ulrich, P., Westerhaus, M., Zippelt, K., 2013. Recent surface displacements in the Upper Rhine Graben — preliminary results from geodetic networks. Tectonophysics, TOPO-EUROPE III 602, 300–315. https://doi.org/10.1016/j.tecto.2012.10.012.

Fuhrmann, T., Caro Cuenca, M., Knöpfler, A., Van Leijen, F., Mayer, M., Westerhaus, M., Hanssen, R., Heck, B., 2015. Combining InSAR, levelling and GNSS for the estimation of 3D surface displacements. In: Proceedings of Fringe 2015: Advances in the Science and Applications of SAR Interferometry and Sentinel-1 InSAR Workshop. Presented at the Fringe2015: Advances in the Science and Applications of SAR Interferometry and Sentinel-1 InSAR Workshop. European Space Agency. https://doi.org/10.5270/Fringe2015.pp80.

Gabriel, G., Ellwanger, D., Hoselmann, C., Weidenfeller, M., Wielandt-Schuster, U., The Heidelberg Basin Project Team, 2013. The Heidelberg Basin, upper rhine graben (Germany): a unique archive of quaternary sediments in central Europe. Quat. Int. 292, 43–58. https://doi.org/10.1016/j.quaint.2012.10.044.

Gegg, L., Griebling, F.A., Jentz, N., Wieland-Schuster, U., in review. Towards a quantitative lithostratigraphy of Pleistocene fluvial deposits in the southern Upper Rhine Graben. E&G Quaternary Science Journal.

Geissert, F., 1967. Fossile Pflanzenreste und Mollusken aus dem Tonlager von Jockgrim in der Pfalz. Mitteilungen des Badischen Landesvereins für Naturkunde und Naturschutz e.V. Freiburg i. Br. NF 9, 443–458.

GeORG-Projektteam, 2013. Geopotenziale des tieferen Untergrundes im Oberrheingraben, Fachlich-Technischer Abschlussbericht des INTERREG-Projekts GeORG, Teil 1: Zusammenfassung. LGRB Info 28, 103.

Georgopoulou, E., Neubauer, T.A., Kroh, A., Harzhauser, M., Mandic, O., others, 2015. An outline of the European Quaternary localities with freshwater gastropods: data on geography and updated stratigraphy. Palaeontol. Electron. 18 (3.48A), 1–9.

Germain, L., 1930. Mollusques terrestres et fluviatiles (première partie). P. Lechevalier, Paris.

Germain, L., 1931. Mollusques terrestres et fluviatiles (deuxième partie). P. Lechevalier, Paris.

Geyer, M., Nitsch, E., Simon, T., Geyer, O.F., Gwinner, M.P., 2011. Geologie von Baden-Württemberg, fifth ed. Schweizerbart'sche, E., Stuttgart.

Geyh, M.A., Müller, H., 2005. Numerical 230Th/U dating and a palynological review of the Holsteinian/Hoxnian Interglacial. Quat. Sci. Rev. 24, 1861–1872. https://doi.org/10.1016/j.quascirev.2005.01.007.

Gibbard, P.L., Clark, C.D., 2011. Pleistocene glaciation limits in great britain. In: Developments in Quaternary Sciences. Elsevier, pp. 75–93.

Gibbard, P.L., Hughes, P.D., 2021. Terrestrial stratigraphical division in the Quaternary and its correlation. J. Geol. Soc. 178, jgs2020–j2134.

Gilbertson, D.D., Hawkins, A.B., 1978. The pleistocene succession at kenn, Somerset. H. M. Stationery Office, 49 pp.

Gittenberger, E., Janssen, A.W., Kuijper, W.J., de Bruyne, R.H., Cadee, M.C., Wallbrink, H., 1998. Nederlandse zoetwatermollusken: recente en fossiele weekdieren uit zoet en brak water | Hydrotheek. Nederlandse Fauna. KNVV, Utrecht.

Grüger, E., 1967. Vegetationsgeschichtliche Untersuchungen an cromer-zeitlichen Ablagerungen im nördlichen Randgebiet der deutschen Mittelgebirge. E&G Quaternary Science Journal 18, 204–235. https://doi.org/10.3285/eg.18.1.14.

Grüger, E., 1983. Untersuchungen zur Gliederung und Vegetationsgeschichte des Mittelpleistozäns am Samerberg in Oberbayern. Geol. Bavarica 84, 21–40.

Hagedorn, E.M., Boenigk, W., 2008. The Pliocene and Quaternary sedimentary and fluvial history in the Upper Rhine Graben based on heavy mineral analyses. Netherlands Journal of Geosciences-Geologie en Mijnbouw 87, 21–32. https://doi.org/10.1017/S001677460002401X.

Hahne, J., 1996. The interglacial site of Hunteburg near Quakenbrück (NW Germany). In: The Early Middle Pleistocene in Europe. CRC Press.

Hahne, J., Mengeling, H., Merkt, J., Gramann, F., 1994. Die Hunteburg-Warmzeit ("Cromer-Komplex") und Ablagerungen der Elster-, Saale- und Weichsel-Kaltzeit in der Forschungsbohrung Hunteburg GE 58 bei Osnabrück. Geol. Jahrb. 134, 117–166.

Hahne, J., Ellwanger, D., Franz, M., Stritzke, R., Wielandt-Schuster, U., 2012. Pollenanalytische Untersuchungsergebnisse aus dem baden-württembergischen Rheinsystem Oberrheingraben, Hochrhein, Oberschwaben – eine Zusammenfassung des aktuellen Kenntnisstandes. LGRB Informationen 26, 119–154.

Hammer, Ø., Harper, D.A.T., Ryan, P.D., 2001. PAST: paleontological statistics software package for education and data analysis. Palaeontol. Electron. 4, 9.

Hare, P.E., Mitterer, R.M., 1968. Laboratory simulations of amino acid diagenesis in fossils. In: Carnegie Institute Year Book, pp. 205–212.

Head, M.J., Gibbard, P.L., 2005. Early-Middle Pleistocene Transitions: an Overview and Recommendation for the Defining Boundary, vol. 247. Geological Society, London, Special Publications, pp. 1–18. https://doi.org/10.1144/GSL.SP.2005.247.01.01.

Heiri, O., Lotter, A.F., Lemcke, G., 2001. Loss on ignition as a method for estimating organic and carbonate content in sediments: reproducibility and comparability of results. J. Paleolimnol. 25, 101–110. https://doi.org/10.1023/A:1008119611481.

Hill, R.L., 1965. Hydrolysis of proteins. In: Anfinsen, C.B., Anson, M.L., Edsall, J.T., Richards, F.M. (Eds.), Advances in Protein Chemistry. Academic Press, pp. 37–107. https://doi.org/10.1016/S0065-3233(08)60388-5.

Holland, S.M., 2016. The non-uniformity of fossil preservation. Phil. Trans. Biol. Sci. 371, 20150130. https://doi.org/10.1098/rstb.2015.0130.

Horsák, M., Juřičková, L., Picka, J., 2013. Měkkýši České a Slovenské republiky. Kabourek, Zlín.

Hošek, J., Pokorný, P., Storch, D., Kvaček, J., Havig, J., Novák, J., Hájková, P., Jamrichová, E., Brengman, L., Radoměřský, T., Křížek, M., Magna, T., Rapprich, V., Laufek, F., Hamilton, T., Pack, A., di Rocco, T., Horáček, I., 2024. Hot spring oases in the periglacial desert as the Last Glacial Maximum refugia for temperate trees in Central Europe. Sci. Adv. 10, eado6611. https://doi.org/10.1126/sciadv.ado6611.

Hoselmann, C., 2009. The Pliocene and Pleistocene fluvial evolution in the northern Upper Rhine Graben based on results of the research borehole at Viernheim (Hessen, Germany). E&G Quaternary Sci. J. 57 (2), 286–314. https://doi.org/10.3285/eg.57.3-4.

Hughes, P.D., Gibbard, P.L., Ehlers, J., 2019. The "missing glaciations" of the Middle Pleistocene. Quaternary Research 96, 161–183. https://doi.org/10.1017/qua.2019.76.

Jansen, E., Overpeck, J., Briffa, K.R., Duplessy, J.-C., Joos, F., Masson-Delmotte, V., Olago, D., Otto-Bliesner, B., Peltier, W.R., Rahmstorf, S., Ramesh, R., Raynaud, D., Rind, D., Solomina, O., Villalba, R., Zhang, D., Barnola, J.-M., Bauer, E., Brady, E., Chandler, M., Cole, J., Cook, E., Cortijo, E., Dokken, T., Fleitmann, D., Kageyama, M., Khodri, M., Labeyrie, L., Laine, A., Levermann, A., Lie, Ø., Loutre, M.-F., Matsumoto, K., Monnin, E., Mosley-Thompson, E., Muhs, D., Muscheler, R., Osborn, T., Paasche, Ø., Parrenin, F., Plattner, G.-K., Pollack, H., Spahni, R., Stott, L. D., Thompson, L., Waelbroeck, C., Wiles, G., Zachos, J., Zhengteng, G., Jouzel, J., Mitchell, J., Solomon, S., Qin, D., Manning, M., Chen, Z., Marquis, M., Averyt, K.B., Tignor, M., Miller, H.L., 2007. Palaeoclimate. In: Solomon, S., Qin, D., Manning, M., Chen, Z., Marquis, M., Averyt, K.B., Tignor, M., Miller, H.L. (Eds.), Contribution of Working Group I to the Fourth Assessment Report of the Intergovernmental Panel on Climate Change. Cambridge University Press.

Karcz, I., 1969. Mud pebbles in a flash floods environment. J. Sediment. Res. 39, 333–337. https://doi.org/10.1306/74D71C53-2B21-11D7-8648000102C1865D.

Kaufman, D.S., Manley, W.F., 1998. A new procedure for determining dl amino acid ratios in fossils using reverse phase liquid chromatography. Quat. Sci. Rev. 17, 987. https://doi.org/10.1016/S0277-3791(97)00086-3, 100.

Keilhack, K., 1915. Das glaziale Diluvium der mittleren Niederlande. Jahrbuch der Königlichen Preussischen Geologischen Landesanstalt zu. Berlin 36, 458–497.

Kerney, M.P., Cameron, R.A.D., Jungbluth, J.H., 1983. Die Landschnecken Nord- und Mitteleuropas. Ein Bestimmungsbuch für Biologen und Naturfreunde. Paul Parey, Hamburg, Berlin.

Knipping, M., 2008. Early and Middle Pleistocene pollen assemblages of deep core drillings in the northern Upper Rhine Graben, Germany. Neth. J. Geosci. 87, 51–65. https://doi.org/10.1017/S0016774600024045.

Koltzer, N., Scheck-Wenderoth, M., Cacace, M., Frick, M., Bott, J., 2019. Regional hydraulic model of the upper rhine graben. In: Advances in Geosciences. Presented at the EGU General Assembly 2019, Vienna, pp. 197–206. https://doi.org/10.5194/adgeo-49-197-2019.

Kolumbe, E., 1960. Pollenanalytische Untersuchungen an Interglazialen im Raum von Karlsruhe. E&G Quaternary Science Journal 11, 227–228.

Kühl, N., Gobet, E., 2010. Climatic evolution during the middle pleistocene warm period of bilshausen, Germany, compared to the Holocene. Quat. Sci. Rev. 29, 3736–3749. https://doi.org/10.1016/j.quascirev.2010.08.006.

Kukla, G., 2003. Continental records of MIS 11. Geophys. Monogr. 137, 207–211. https://doi.org/10.1029/137GM14.

Lang, S., Hornung, J.M.K., Ruckwied, K., Hoppe, A., 2011. Tektonik und Sedimentation am Rand des Oberrheingrabens in Darmstadt im Mittel- und Oberpleistozän. Geol. Jahrb. Hessen 137, 19–53.

Lauer, T., Weiss, M., 2018. Timing of the Saalian- and Elsterian glacial cycles and the implications for Middle – pleistocene hominin presence in central Europe. Sci. Rep. 8, 5111. https://doi.org/10.1038/s41598-018-23541-w.

Lauer, T., Frechen, M., Hoselmann, C., Tsukamoto, S., 2010. Fluvial aggradation phases in the Upper Rhine Graben — new insights by quartz OSL dating. PGA (Proc. Geol. Assoc.) 121, 154–161. https://doi.org/10.1016/j.pgeola.2009.10.006.

Lauer, T., Krbetschek, M., Frechen, M., Tsukamoto, S., Hoselmann, C., Weidenfeller, M., 2011. Infrared radiofluorescence (IR-RF) dating of middle pleistocene fluvial archives of the Heidelberg Basin (Southwest Germany). Geochron 38, 23–33. https://doi.org/10.2478/s13386-011-0006-9.

Lauer, T., Stahlschmidt, M., Penkman, K.E.H., Daniel, T., Heinrich, S., Pasda, C., 2021. The Middle Pleistocene site of Bilzingsleben - new insights into chronology and site formation. Presented at the vDEUQUA 2021 - German Quaternary Conference 2021.

Leeder, M.R., Harris, T., Kirkby, M.J., 1998. Sediment supply and climate change: implications for basin stratigraphy. Basin Res. 10, 7–18. https://doi.org/10.1046/j.1365-2117.1998.00054.x.

Leipe, C., Kobe, F., Müller, S., 2019. Testing the performance of sodium polytungstate and lithium heteropolytungstate as non-toxic dense media for pollen extraction from lake and peat sediment samples. Quat. Int. 516, 207–214. https://doi.org/10.1016/j.quaint.2018.01.029.

Li, B., Li, S.-H., 2011. Luminescence dating of K-feldspar from sediments: a protocol without anomalous fading correction. Quat. Geochronol. 6, 468–479. https://doi.org/10.1016/j.quageo.2011.05.001.

Li, Y., Tsukamoto, S., Frechen, M., Gabriel, G., 2018. Timing of fluvial sedimentation in the Upper Rhine Graben since the Middle Pleistocene: constraints from quartz and feldspar luminescence dating. Boreas 47, 256–270.

Limondin-Lozouet, N., 1998. Successions malacologiques du Tardiglaciaire weichsélien : Corrélations entre séries du Nord de la France et du Sud-Est de la Grande-Bretagne. Quaternaire 9, 217–225. https://doi.org/10.3406/quate.1998.1604.

Limondin-Lozouet, N., 2002. Impact des oscillations climatiques du Tardiglaciaire sur l'évolution des malacofaunes de fond de vallée en Europe du Nord-Ouest. Annales littéraires de l'Université de Besançon 730, 45–51.

Limondin-Lozouet, N., Preece, R.C., 2014. Quaternary perspectives on the diversity of land snail assemblages from northwestern Europe. J. Molluscan Stud. 80, 224–237. https://doi.org/10.1093/mollus/eyu047.

Lisiecki, L.E., Raymo, M.E., 2005. A Pliocene-Pleistocene stack of 57 globally distributed benthic δ 18 O records. Paleoceanography 20. https://doi.org/10.1029/2004PA001071, 2004PA001071.

Litt, T., Behre, K.-E., Meyer, K.-D., Stephan, H.-J., Wansa, S., 2007. Stratigraphische Begriffe für das Quartär des norddeutschen Vereisungsgebietes. E&G Quaternary Science Journal 56, 7–65. https://doi.org/10.3285/eg.56.1-2.02.

Löscher, M., Becker, B., Bruns, M., Hieronymus, U., Mäusbacher, R., Münnich, M., Münzing, K., Schedler, J., 1980. Neue Ergebnisse über das Jungquartär im Neckarschwemmfächer bei Heidelberg. E&G Quaternary Science Journal 30, 89–100. https://doi.org/10.3285/eg.30.1.07.

Ložek, V., 1964. Quartärmollusken der Tschechoslowakei, Rozpravy Ústredního ústuvu geologického. Prague.

Marcussen, I., 1967. The freshwater molluscs in the Late-glacial and early Post-glacial deposits in the bog of Barmosen, southern Sjælland, Denmark. Med. Dan. Geol. Foren. 17, 265–283.

Maul, L.C., Stebich, M., Frenzel, P., Hambach, U., Henkel, T., Katzschmann, L., Kienast, F., Meng, S., Penkman, K., Rolf, C., Thomas, M., Kahlke, R.-D., 2013. Age and palaeoenvironment of the enigmatic arternian interglacial — evidence from the muschelton at voigtstedt/hackelsberg (Thuringia, Central Germany). Palaeogeogr. Palaeoclimatol. Palaeoecol. 386, 68–85. https://doi.org/10.1016/j.palaeo.2013.05.005.

Meijer, T., 1989. Notes on Quaternary freshwater Mollusca of The Netherlands, with description of some new species. Meded. Werkgr. Tert. Kwart. Geol. 26, 145–181.

Meinken, W., Stober, I., 1997. Permeability distribution in the quaternary of the upper rhine glacio-fluvial aquifer. Terra. Nova 9, 113–116. https://doi.org/10.1046/j.1365-3121.1997.d01-16.x.

Menzies, J., Ellwanger, D., 2015. Climate and paleo-environmental change within the Mannheim Formation near Heidelberg, Upper Rhine Valley, Germany: a case study based upon microsedimentological analyses. Quat. Int. 386, 137–147. https://doi.org/10.1016/j.quaint.2015.03.037.

Merritts, D.J., Rahnis, M.A., 2022. Pleistocene periglacial processes and landforms, mid-atlantic region, eastern United States. Annu. Rev. Earth Planet Sci. 50, 541–592. https://doi.org/10.1146/annurev-earth-032320-102849.

Meyer, M., Palkopoulou, E., Baleka, S., Stiller, M., Penkman, K.E.H., Alt, K.W., Ishida, Y., Mania, D., Mallick, S., Meijer, T., Meller, H., Nagel, S., Nickel, B., Ostritz, S., Rohland, N., Schauer, K., Schüler, T., Roca, A.L., Reich, D., Shapiro, B., Hofreiter, M., 2017. Palaeogenomes of Eurasian straight-tusked elephants challenge the current view of elephant evolution. Elife 6, e25413. https://doi.org/10.7554/eLife.25413.

Miller, G.H., Magee, J.W., Johnson, B.J., Fogel, M.L., Spooner, N.A., McCulloch, M.T., Ayliffe, L.K., 1999. Pleistocene extinction of genyornis newtoni: human impact on Australian megafauna. Science 283, 205–208. https://doi.org/10.1126/science.283.5399.205.

Moine, O., 2014. Weichselian Upper Pleniglacial environmental variability in north-western Europe reconstructed from terrestrial mollusc faunas and its relationship with the presence/absence of human settlements. Quaternary International, Environmental and Cultural Dynamics in Western and Central Europe during the Upper Pleistocene 337, 90–113. https://doi.org/10.1016/j.quaint.2014.02.030.

Mueller, D., Preusser, F., Buechi, M.W., Gegg, L., Deplazes, G., 2020. Luminescence properties and dating of glacial to periglacial sediments from northern Switzerland. Geochronology 2, 305–323. https://doi.org/10.5194/gchron-2-305-2020.

Müller, H., 1965. Eine pollenanalytische Neubearbeitung des Interglazialprofils von Bilshausen. Geol. Jahrb. 83, 327–352.

Müller, H., 1992. Climate changes during and at the end of the interglacials of the cromerian complex. In: Kukla, G.J., Went, E. (Eds.), Start of a Glacial, NATO ASI Series. Springer, Berlin, Heidelberg, pp. 51–69. https://doi.org/10.1007/978-3-642-76954-2_5.

Müller-Stoll, W.R., 1985. Pollenanalytische Untersuchung des altpleistozänen Tonlagers von Jockgrim (Rheinpfalz). Carolinea 42, 9–29.

Münzing, K., 1969. Quartäre Molluskenfaunen aus dem Kaiserstuhl. Jahreshefte Geol. Landesamtes Baden-Wurttemberg 11, 87–115.

Münzing, K., 1976. Zur Stratigraphie der Breisgauer Lösse (Südbaden). Mitteilungen des Badischen Landesvereins für Naturkunde und Naturschutz e. V. 11, 257–272.

Pena-Castellnou, S., Hürtgen, J., Baize, S., Preusser, F., Mueller, D., Jomard, H., Cushing, E.M., Rockwell, T.K., Seitz, G., Cinti, F.R., Ritter, J., Reicherter, K., 2023. Surface rupturing earthquakes along the eastern rhine graben boundary fault near ettlingen-oberweier (Germany). Tectonophysics 869, 230114. https://doi.org/10.1016/j.tecto.2023.230114.

Penck, A., Brückner, E., 1909. Die Alpen im Eiszeitalter. Tauchnitz, Leipzig.

Penkman, K.E.H., 2010. Neumark-Nord 1: preliminary results of the amino acid analysis. In: Meller, H. (Ed.), Elefantenreich - Eine Fossilwelt in Europa. Landesamt für Denkmalpflege une Archäologie Sachsen-Anhalt – Landesmuseum für Vorgeschichte, pp. 75–78.

Penkman, K.E.H., Kaufman, D.S., Maddy, D., Collins, M.J., 2008. Closed-system behaviour of the intra-crystalline fraction of amino acids in mollusc shells. Quat. Geochronol. 3, 2–25. https://doi.org/10.1016/j.quageo.2007.07.001.

Penkman, K.E.H., Preece, R.C., Bridgland, D.R., Keen, D.H., Meijer, T., Parfitt, S.A., White, T.S., Collins, M.J., 2011. A chronological framework for the British Quaternary based on Bithynia opercula. Nature 476, 446–449. https://doi.org/10.1038/nature10305.

Penkman, K.E.H., Preece, R.C., Bridgland, D.R., Keen, D.H., Meijer, T., Parfitt, S.A., White, T.S., Collins, M.J., 2013. An aminostratigraphy for the British Quaternary based on Bithynia opercula. Quat. Sci. Rev. 61, 111–134. https://doi.org/10.1016/j.quascirev.2012.10.046.

Peters, I., 1965. Zur Altersstellung der Torfe und Gyttjen von Herxheim, Jockgrim und Rheinzabern in der Vorderpfalz. E&G – Quaternary Science Journal 16, 121–131. https://doi.org/10.3285/eg.16.1.12.

Pfiffner, O.A., 2010. Geologie der Alpen. UTB Geologie, second ed. Haupt Verlag, Bern.

Powers, M.C., 1953. A new roundness scale for sedimentary particles. SEPM JSR 23. https://doi.org/10.1306/D4269567-2B26-11D7-8648000102C1865D.

Preece, R.C., Penkman, K.E.H., 2005. New faunal analyses and amino acid dating of the lower palaeolithic site at east farm, barnham, suffolk. Proceedings of the Geologists' Association, Commemorating the life and work of Douglas Shearman, 1918–2003 116, 363–377. https://doi.org/10.1016/S0016-7878(05)80053-7.

Preusser, F., 2008. Characterisation and evolution of the river rhine system. Neth. J. Geosci. 87, 7–19. https://doi.org/10.1017/S0016774600024008.

Preusser, F., Graf, H.R., Keller, O., Krayss, E., Schlüchter, C., 2011. Quaternary glaciation history of northern Switzerland. E&G Quaternary Science Journal 60, 282–305.

Preusser, F., Büschelberger, M., Kemna, H.A., Miocic, J., Mueller, D., May, J.-H., 2021. Exploring possible links between Quaternary aggradation in the Upper Rhine Graben and the glaciation history of northern Switzerland. Int. J. Earth Sci. 1–20. https://doi.org/10.1007/s00531-021-02043-7.

Preusser, F., Degering, D., Fülling, A., Miocic, J., 2023. Complex dose rate calculations in luminescence dating of lacustrine and palustrine sediments from niederweningen, northern Switzerland. Geochronometria 50, 28–49.

Przyrowski, R., Schäfer, A., 2015. Quaternary fluvial basin of northern upper rhine graben. Z. Dtsch. Ges. Geowiss. 166, 71–98. https://doi.org/10.1127/1860-1804/2014/0080.

Puisségur, J.-J.A., 1976. Mollusques continentaux quaternaires de Bourgogne: significations stratigraphiques et climatiques, rapports avec d'autres faunes boréales en France. Doin.

Rähle, W., 2005. Eine mittelpleistozäne Molluskenfauna aus dem Oberen Zwischenhorizont des nördlichen Oberrheingrabens (Bohrung Mannheim-Lindenhof). Mainz. Geowiss. Mitt. 33, 9–20.

Reiff, W., 1965. Das Alter der Sauerwasserkalke von Stuttgart - Münster - Bad Cannstatt - Untertürkheim. Jahresber. Mittl. Oberrheinischen Geol. Vereins 111–134. https://doi.org/10.1127/jmogv/47/1965/111.

Reille, M., 1998. Pollen et spores d'Europe et d'Afrique du Nord. Laboratoire de Botanique historique et Palynologie, Marseille.

Richter, D., Richter, A., Dornich, K., 2015. Lexsyg smart - a luminescence detection system for dosimetry, material research and dating application. Geochronometria 42, 202–209. https://doi.org/10.1515/geochr-2015-0022.

Richter, D., Woda, C., Dornich, K., 2020. A new quartz for γ-transfer calibration of radiation sources. Geochronometria 47, 23–34. https://doi.org/10.2478/geochr-2020-0020.

Ritter, J.R.R., Wagner, M., Bonjer, K.-P., Schmidt, B., 2009. The 2005 Heidelberg and Speyer earthquakes and their relationship to active tectonics in the central Upper Rhine Graben. Int. J. Earth Sci. 98, 697–705. https://doi.org/10.1007/s00531-007-0284-x.

Scheidt, S., Hambach, U., Rolf, C., 2015. A consistent magnetic polarity stratigraphy of late Neogene to Quaternary fluvial sediments from the Heidelberg Basin (Germany): a new time frame for the Plio–Pleistocene palaeoclimatic evolution of the Rhine Basin. Global Planet. Change 127, 103–116. https://doi.org/10.1016/j.gloplacha.2015.01.004.

Schileyko, A.A., 1984. Land mollusc suborder pupillina of USSR fauna (gastropoda, pulmonata, geophila), fauna of the USSR. New Series. Nauka, Leningrad.

Schloss, S., 2012. Ein Eem-zeitliches Pollenprofil aus der Nördlichen Oberrheinniederung bei Philippsburg. LGRB Informationen 26, 155–162.

Schlüchter, C., 1992. Terrestrial quaternary stratigraphy. Quat. Sci. Rev. 11, 603–607. https://doi.org/10.1016/0277-3791(92)90017-3.

Schlüchter, C., Akçar, N., Ivy-Ochs, S., 2021. The quaternary period in Switzerland. In: Landscapes and Landforms of Switzerland. Springer, pp. 47–69.

Schmidt, C., Friedrich, J., Adamiec, G., Chruścińska, A., Fasoli, M., Kreutzer, S., Martini, M., Panzeri, L., Polymeris, G.S., Przegiętka, K., Valla, P.G., King, G.E., Sanderson, D.C.W., 2018. How reproducible are kinetic parameter constraints of quartz luminescence? An interlaboratory comparison for the 110 °C TL peak. Radiat. Meas. 110, 14–24. https://doi.org/10.1016/j.radmeas.2018.01.002.

Schulze, T., Schwahn, L., Fülling, A., Zeeden, C., Preusser, F., Sprafke, T., 2022. Investigating the loess–palaeosol sequence of Bahlingen-Schönenberg (Kaiserstuhl), southwestern Germany, using a multi-methodological approach. E&G Quaternary Science Journal 71, 145–162. https://doi.org/10.5194/egqsj-71-145-2022.

Schwahn, L., Schulze, T., Fülling, A., Zeeden, C., Preusser, F., Sprafke, T., 2023. Multi-method study of the Middle Pleistocene loess–palaeosol sequence of Köndringen, SW Germany. E&G Quaternary Sci. J. 72, 1–21. https://doi.org/10.5194/egqsj-72-1-2023.

Scourse, J., 2006. Comment on: numerical ²³⁰Th/U dating and a palynological review of the holsteinian/hoxnian interglacial by Geyh and müller. Quat. Sci. Rev. 25, 3070–3071. https://doi.org/10.1016/j.quascirev.2006.03.006.

Sier, M.J., Roebroeks, W., Bakels, C.C., Dekkers, M.J., Brühl, E., De Loecker, D., Gaudzinski-Windheuser, S., Hesse, N., Jagich, A., Kindler, L., Kuijper, W.J., Laurat, T., Mücher, H.J., Penkman, K.E.H., Richter, D., van Hinsbergen, D.J.J., 2011. Direct terrestrial–marine correlation demonstrates surprisingly late onset of the last interglacial in central Europe. Quaternary Research 75, 213–218. https://doi.org/10.1016/j.yqres.2010.11.003.

Simon, T., 2012. Herkunft und Transport der Sedimente in der Forschungsbohrung Heidelberg UniNord. LGRB Informationen 26, 107–118.

Skompski, S., 1982. Correlation of the mazovian interglacial of western Poland with the holstein interglacial of the eastern part of German democratic republic. Biul. Panstwowego Inst. Geol. (1989) 343, 51–58.

Skrzypek, E., Schulmann, K., Tabaud, A.-S., Edel, J.-B., 2014. Palaeozoic Evolution of the Variscan Vosges Mountains, vol. 405. Geological Society, London, Special Publications, pp. 45–75. https://doi.org/10.1144/SP405.8.

Stober, I., Bucher, K., 2015. Hydraulic and hydrochemical properties of deep sedimentary reservoirs of the Upper Rhine Graben, Europe. Geofluids 15, 464–482. https://doi.org/10.1111/gfl.12122.

Szymanek, M., Julien, M.-A., 2018. Early and Middle Pleistocene climate-environment conditions in Central Europe and the hominin settlement record. Quat. Sci. Rev. 198, 56–75. https://doi.org/10.1016/j.quascirev.2018.08.021.

Tesakov, A.S., Frolov, P.D., Titov, V.V., Dickinson, M., Meijer, T., Parfitt, S.A., Preece, R. C., Penkman, K.E.H., 2020. Aminostratigraphical test of the East European mammal zonation for the late neogene and quaternary. Quat. Sci. Rev. 245, 106434. https://doi.org/10.1016/j.quascirev.2020.106434.

Urban, B., 1983. Biostratigraphic correlation of the Kärlich interglacial, northwestern Germany. Boreas 12, 83–90. https://doi.org/10.1111/j.1502-3885.1983.tb00440.x.

Van Den Bogaard, C., Van Den Bogaard, P., Schmincke, H.-U., 1989. Quartärgeologisch-tephrostratigraphische Neuaufnahme und Interpretation des Pleistozänprofils Kärlich. E&G Quaternary Science Journal 39, 62–86. https://doi.org/10.3285/eg.39.1.08.

Vereș, D., 2002. A comparative study between loss on ignition and total carbon analysis on mineralogenic sediments. Studia UBB Geologia 47, 171–182. https://doi.org/10.5038/1937-8602.47.1.13.

von der Brelie, G., 1982. Pollenuntersuchungen. In: Bartz, J. (Ed.), Quartär Und Jungtertiär II Im Oberrheingraben Im Großraum Karlsruhe, Geologische Jahrbuch Reihe A, pp. 199–227.

Wedel, J., 2009. Pleistocene molluscs from research boreholes in the Heidelberg Basin. E&G Quaternary Science Journal 57 (6), 382–402. https://doi.org/10.3285/eg.57.3-4.

Wehmiller, J.F., Stecher, H., York, L.A., Friedman, I., 2000. The thermal environment of fossils: effective ground temperatures at aminostratigraphic sites on the U.S. Coastal Plain. In: Goodfriend, G.A., Collins, M.J., Fogel, M.L., Macko, S.A., Wehmiller, J.F. (Eds.), Perspectives in Amino Acid and Protein Geochemistry. Oxford University Press, pp. 219–250.

Weidenfeller, M., Kärcher, T., 2008. Tectonic influence on fluvial preservation: aspects of the architecture of Middle and Late Pleistocene sediments in the northern Upper Rhine Graben, Germany. Neth. J. Geosci. 87, 33–40. https://doi.org/10.1017/S0016774600024021.

Weidenfeller, M., Knipping, M., 2009. Correlation of pleistocene sediments from boreholes in the ludwigshafen area, western Heidelberg Basin. E&G Quaternary Science Journal 57 (1), 270–285. https://doi.org/10.3285/eg.57.3-4.

Welter-Schultes, F.W. (Ed.), 2012. European non-marine molluscs: a guide for species identification = Bestimmungsbuch für europäische Land- und Süsswassermollusken, 1. ed. ed. Planet Poster Ed. Göttingen.

Wesenberg-Lund, C., Sand, M.J., Boye Petersen, J., Seidelin Rundkiaer, A., Steenberg, C. M., 1917. Furesøstudier. En bathymetrisk botanisk zoologisk Undersøgelse af Mølleaaens Søer. Det Kongelige Danske Videnskabernes Selskabs Skrifter 3, 1–208.

White, D., Preece, R.C., Shchetnikov, A.A., Parfitt, S.A., Dlussky, K.G., 2008. A Holocene molluscan succession from floodplain sediments of the upper Lena River (Lake Baikal region), Siberia. Quat. Sci. Rev. 27, 962–987. https://doi.org/10.1016/j.quascirev.2008.01.010.

White, D., Preece, R.C., Shchetnikov, A.A., Dlussky, K.G., 2013. Late glacial and Holocene environmental change reconstructed from floodplain and aeolian sediments near burdukovo, lower Selenga river valley (lake baikal region), siberia. Quaternary International, The Baikal-Hokkaido Archaeology Project: Environmental archives, proxies and reconstruction approaches 290–291, 68–81. https://doi.org/10.1016/j.quaint.2012.11.007.

Wirsing, G., Luz, A., 2007. Hydrogeologischer Bau und Aquifereigenschaften der Lockergesteine im Oberrheingraben (Baden-Württemberg), vol. 19. LGRB Informationen.

Wriedt, T., 2012. Mie theory: a review. In: Hergert, W., Wriedt, T. (Eds.), The Mie Theory: Basics and Applications, Springer Series in Optical Sciences. Springer, Berlin, Heidelberg, pp. 53–71.

Zagwijn, W.H., 1985. An outline of the Quaternary stratigraphy of the Netherlands. Geologie en Mijnbouw 64, 17-24.Zagwijn, W.H., De Jong, J., 1984. Die Interglaziale von Bavel und Leerdam und ihre stratigraphische Stellung im Niederländischen Früh-Pleistozän. Meded. Rijks Geol. Dienst 37, 156–169.

Ziegler, P.A., 1992. European Cenozoic rift system. Tectonophysics 208, 91–111. https://doi.org/10.1016/0040-1951(92)90338-7.